TABLE OF CONTENTS

TABLE OF CONTENTS - Continued

LIST OF ILLUSTRATIONS

LIST OF ILLUSTRATIONS - Continued

LIST OF TABLES

1. SUMMARY

1.1 Project Objective

The objective of this project is to explore the feasibility of a liquid propellant traveling charge gun concept, which has been proposed as a means for improving the performance of high velocity guns. The concept is based upon a mechanical adaptation of the Taylor theory of cavity formation as a means for both controlling the propellant burning rate and achieving a down-bore traveling charge effect in bulk loaded guns. Improved control over the ballistic process is the objective. Achieving it should broaden the applicability of liquid propellants and permit their advantages to be more successfully exploited.

This report describes a twelve month exploratory study of the traveling charge concept. The study consists of three tasks:

1. Analysis and design of the cavity generator
2. Construction of a single-shot 30mm test fixture and exploratory firings
3. Refinement of the interior ballistic analysis to more accurately predict performance

1.2 Task 1 – Cavity Generator Study

The first step was to establish a design for the cavity generator. The simplified analysis which formed the basis of the preproposal study was modified to suit defined program parameters. The original study had assumed the cavity generator to be a solid displacement body. Hollow shell construction seemed more practical, and the analysis was adapted to consider this type of configuration. A 30mm bore diameter and a 120 gram projectile weight were factored into the analysis. Propellant parameters were changed to those characterizing NOS365 monopropellant, the propellant selected for testing.

An ellipsoid was originally selected as the basic shape for the cavity generators. PH13-8 Mo stainless steel was selected as the material from which they would be fabricated. The combination of properties of high strength, compatibility with NOS365 propellant, and machinability led to the selection of this material.

Calculations were carried out for a wide range of operating conditions. From the results, three representative cavity generator configurations were selected for testing. Designs were adopted which should give fairly wide variation in performance.

In fabricating cavity generators, the shop found it much easier to work with circular arcs than with ellipsoidal surfaces. After a brief study, the cavity generator design was adjusted to combine a short cylindrical skirt with a tangential circular ogive nose. Test quantities of the three hollow shell designs were machined.

1.3 Task 2 – Single Shot Firing Tests

A single shot test fixture was designed and fabricated. The basic fixture consisted of a 30mm smooth bore barrel mounted resiliently on a structural I beam. A threaded breech plug supported the priming system and the cavity generators for firing. Pressure-actuated needle valves permitted the chamber to be loaded and, if necessary, downloaded from a control position outside the test cell. Firing was controlled from the same remote position.

Test fixture instrumentation included at least one pressure transducer near the breech for measuring chamber pressure, three position sensing stations down-bore to measure projectile passage, and a muzzle wire for recording muzzle exit. Each position sensing station consisted of a light beam emitter/photo-diode detector pair looking across the bore and also a nearby pressure transducer for reading pressure events at that station. Provisions were made for redundancy in measuring muzzle velocity.

Testing began with the hollow shell cavity generators. It quickly became apparent that they did not control burning in the desired manner. While a traveling charge effect appeared to be achieved, burning of the propellant behind the cavity generator was erratic and variable.

A new design was developed for the cavity generator. We hypothesized that insufficient propellant burning surface was generated by the single hollow shell. A new design was developed in the form of a solid displacement body machined from polypropylene. Multiple flow passages were provided to subdivide the propellant more thoroughly and so increase burning surface.

A few new cavity generators were fabricated and introduced into the test program. Test results changed dramatically. Muzzle velocities were higher than expected. and pressure-time curves were much improved. Peak pressures were not excessive

Further variations in cavity generator design were introduced, and firing continued in a study of the effects of cavity generator design upon ballistic performance. The character of ignition and the nature of the subsequent combustion processes were both shown to be sensitive to cavity generator design. Evidence indicates that burning progresses through and ultimately occurs ahead of the cavity generator on the most successful firings. The exact nature of the transition from rear to front is not yet known.

1.4 Task 3 – Analysis Refinement

A simple, idealized model had been first used as a basis for predicting dynamic behavior. The objective of the analysis refinement task was to develop a more realistic simulation of the firing process.

Several changes were introduced into the analysis. The properties of NOS365 monopropellant were introduced as computation constants. The projectile weight was established at 120 grams, and a 30mm bore diameter was included. The original concept of the solid cavity generator of fixed density was changed to consider the hollow, thin-walled shell structure with combustion gas inside. Equations for calculating stress within the cavity generator wall were introduced. Later, the program was again changed to consider the solid displacement cavity generator design.

Compressibility of the liquid charge was factored into the analysis. Finally a flexible burning rate equation was introduced which expresses rate of gas generation as a function of unburned liquid charge, chamber pressure, and projectile position. Proportionality constants and exponents can be adjusted. Other factors later deemed appropriate can also be introduced into this equation.

A check between the refined analysis and actual test results disclosed that the analysis still does not adequately model the actual combustion process. The reason is thought to be that the analysis does not yet include the effects of burning in front of the cavity generator during the firing sequence. Further development is suggested to learn more about this phenomenon.

1.5 Conclusions

The character of propellant ignition and the nature of subsequent combustion in a bulk loaded gun have been shown to be sensitive to cavity generator design. Excellent ballistic performance was achieved on some firings. 5500 feet per second was measured at C/M = 1.0.

More remains to be learned, however. Performance was not uniformly consistent. In successful firings, burning apparently progresses ahead of the cavity generator. The sequence of events through which this occurs is not fully known.

Since further knowledge of cavity generator behavior may provide a key to the control of ballistics in bulk loaded guns, continued work is recommended.

2. INTRODUCTION

The interior ballistics of bulk loaded liquid propellant guns has been the subject of study for a number of years. Theoretical models have been developed for the hydrodynamic and thermodynamic processes in the firing chamber. These models have been applied in explaining and predicting ballistic performance with some degree of success. Nevertheless, the hydrodynamic behavior of the liquid charge, which is a critical factor in the overall firing sequence, remains largely beyond the control of the designer.

This report considers a concept suggested to help resolve this problem. The concept is based upon a mechanical adaptation of the Taylor theory of cavity formation as a means for both controlling the propellant burning rate and achieving a down-bore traveling charge effect.

The traveling charge effect is to be achieved through a subcaliber body of revolution placed at the rear of the liquid charge. Termed the "cavity generator", the body of revolution is designed to penetrate the liquid charge during the combustion process and to control the rate at which propellant is supplied to the combustion zone. Figure 2.1 illustrates the concept. Projectile, propellant charge, and cavity generator are shown at a down-bore position part way through the firing process. Acceleration is to the right. The cavity generator separates the bulk of the liquid charge from the combustion zone behind. Through design, the cavity generator is less dense than the liquid it displaces. The density difference gives rise to a force which causes the cavity generator to move forward into the liquid. As the cavity generator penetrates the charge, propellant flows rearward in a relative sense into the combustion zone. Action continues until penetration is complete and all propellant has been burned.

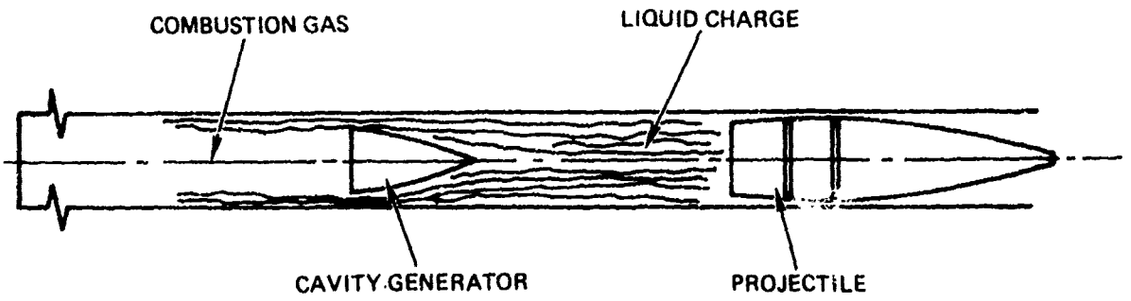

Figure 2.1 Cavity Generator Concept

This concept was proposed in December, 1974, to the Defense Advanced Research Projects Agency by the General Electric Company. In 1975, a contract was established as part of DARPA's Phenomenology Program. The contract called for a ten month study of concept feasibility. The study consisted of three tasks:

1. Analysis and design of the cavity generator
2. Construction of a single-shot 30mm smooth bore test fixture and exploratory firings
3. Refinement of the internal ballistic analysis to more accurately predict performance

The summary of work accomplished is presented in terms of the three individual tasks. Results and conclusions follow. Figure 2.2 is the program schedule. A change in approach after testing had begun occasioned a two month extension at no change in cost.

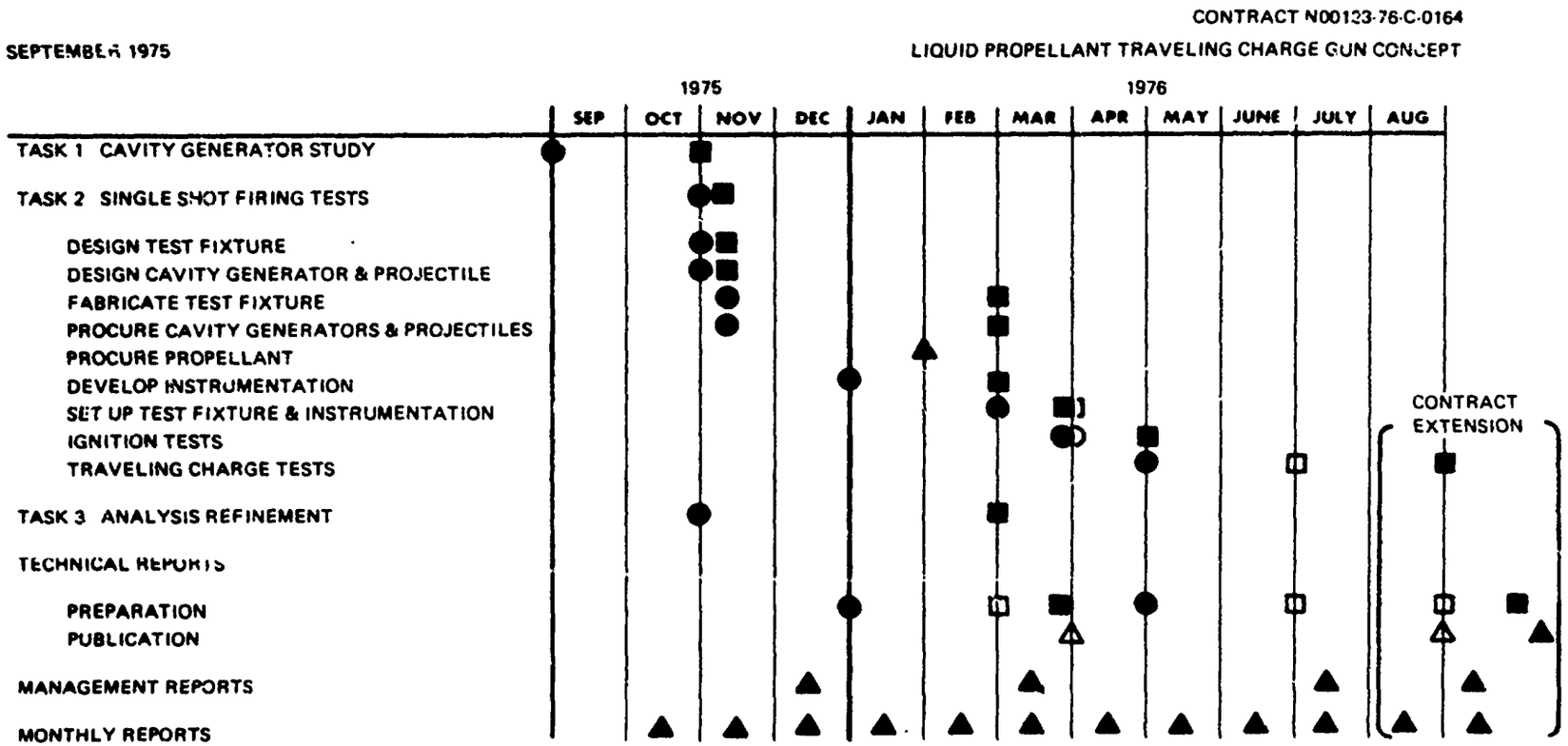

Figure 2.2 Program Schedule

3. TECHNICAL PROGRAM

3.1 Task I – Cavity Generator Study

Two distinctly different types of cavity generators were developed during the program. The original analysis which formed the basis for proposing the cavity generator concept in the first place employed an idealized solid displacement body of .5 specific gravity. As the program began, this approach seemed an oversimplification. In view of the pressure forces and dynamic conditions presumed to be operating, hollow shell construction seemed a more practical approach. Accordingly, a hollow shell configuration was the first design developed and tested.

The first series of firing tests suggested a change, however. Section 3.2 will explain how the hollow shell did not produce the desired results. A second approach was accordingly adopted which followed more closely the original concept of a solid displacement body with multiple liquid passages. The two designs will be considered separately in Sections 3.1.1 and 3.1.2 which follow.

3.1.1 HOLLOW SHELL CAVITY GENERATOR DESIGN

3.1.1.1 Adaptation of Analysis. The first steps necessary in designing a hollow shell cavity generator were to adjust the equations used in dynamic analysis, to select cavity generator configurations, and to apply the iterative computational procedure followed in developing a cavity generator design. In pursuing the discussion it will be helpful to repeat the simplified equation for penetration velocity with which we are working:

$$V_2 = \sqrt{\frac{2AV_{CG}\left(1 - \frac{\rho_{CG}}{\rho_L}\right)}{A_C\left(\frac{A_C^2}{(A_C - A_1)^2} - 1\right)}} \qquad (1)$$

where:

V_2 = penetration velocity

A = projectile acceleration

ρ_{CG} = density of cavity generator

ρ_L = density of liquid propellant

V_{CG} = volume of cavity generator

A_1 = cavity generator base area

A_C = bore area

The density of the cavity generator appears explicitly in the term $(1 - \frac{\rho_{CG}}{\rho_L})$ as a quantity divided by the propellant density. Where ρ_{CG} was originally a constant, it now had to be adjusted to account for the fixed weight of the shell and the varying density of the gas inside. The density term was changed in the computation procedure to an expression which includes both the structural weight of the cavity generator and the gas inside:

$$\bar{\rho}_{CG} = \frac{(V_{CG} - A_S t)\rho_{GAS} + A_S t \rho_{CGW}}{V_{CG}} \qquad (2)$$

where:

A_S = cavity generator surface area

t = cavity generator wall thickness

$\bar{\rho}_{CG}$ = average density of cavity generator

ρ_{CGW} = density of wall material

ρ_{GAS} = density of chamber gas

It then became necessary to choose a configuration and the material for the cavity generator. These involve the parameters A_S, t, and ρ_{CG}, which are physical dimensions and material properties.

An ellipsoid was first selected as the basic shape. Reasoning was as follows: Equation 1 shows that penetration velocity is increased by increasing V_{CG} and reducing ρ_{CG}. This implies that the configuration selected should have as large a volume for as small a surface area as possible. A hemisphere would be the best shape in this respect, but a hemispherical cavity generator seems too short in proportion to its diameter. The next preference would then seem to be an elongated hemisphere, which is an ellipsoid.

Some thought was given to a parabaloid as a shape. As it turns out, the volume per unit surface area of a parabaloid is somewhat less than that for an ellipsoid. For this reason, the parabaloid was not considered further.

Another decision had to be made regarding material, since the density of the cavity generator wall enters into the new equation. High strength stainless steel was selected as the material to be used in the tests. Propellant compatibility and ease of manufacture were the two governing factors. Stainless steel is compatible with NOS365, so we would introduce no problems in this area. Fabricating techniques were our second concern. Ultimately, a more sophisticated construction of fiber reinforced or filament wound plastic may be desirable. These exhibit higher strength-to-weight ratios than even the best stainless steels. However, tooling and the need to develop fabrication techniques would pose problems in a flexible test program. On the other hand, stainless steel can be machined in our own shop with inexpensive tooling, and it would be easy to adjust shape and size for the tests. Complicated development of the more sophisticated version was not considered practical in this program. Feasibility could be demonstrated without developing the ultimate design.

3.1.1.2 Stress Considerations. wall thickness was the last remaining parameter to be selected in designing the cavity generator. Wall thickness controls the weight of the cavity generator, since thickness times area is a measure of its intrinsic volume and hence of its weight. Thickness should be that minimum value which will still keep stress levels within permissible bounds. The iterative nature of the design process now becomes apparent. Selection of thickness determines the weight of the cavity generator. This in turn has a bearing on dynamic performance, which involves chamber pressure and acceleration. These two parameters in turn determine the stress value. Stress is a function of wall thickness. We thus come full circle. A choice in thickness determines stress which in turn requires an adjustment in thickness.

Some concept adjustments were necessary in modeling computations for stress. In normal shell theory, as applied to the analysis of pressure vessels, meridional and tangential principal stresses counteract the effect of internal pressure. Figure 3-1 shows schematically an element of wall subjected to these stresses. Normal analysis sums these stresses on the surface of the shell in determining overall stress distribution.

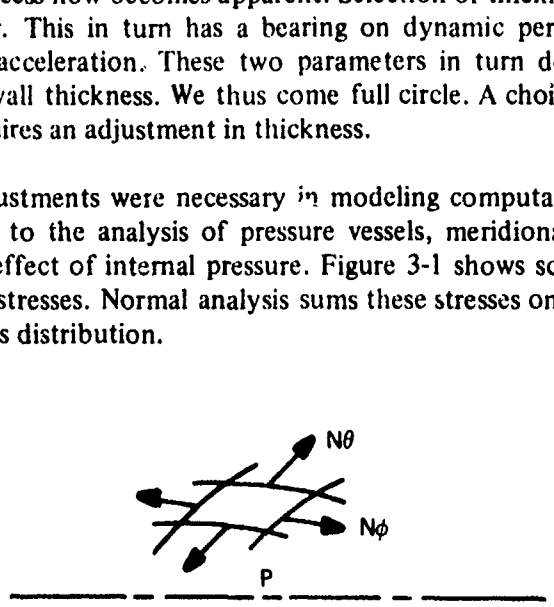

Figure 3.1. Wall Element Stress

The cavity generator is not a complete pressure vessel however. It is open at the rear, and the meridional stress at the trailing edge must be zero.

Thinking back to the original analysis for penetration velocity, the summation of axial wall forces ΣdF_x, has been assumed balanced by fluid pressure against the outward surface of the shell. The shell structure does not restrain the summed axial forces but simply transmits them to the fluid ahead.

This conceptual adjustment was applied in developing an expression for calculating stress in the cavity generator wall. The axial components of pressure forces were neglected and the general equations of shell theory for shells of revolution yielded the following expressions for stress in the wall of an ellipsoidal cavity generator.

$$N_\phi = 0 \tag{3}$$

$$N_\theta = \Delta P \, r_2 \, SIN^2 \, \phi \tag{4}$$

where:

N_ϕ = meridional thin wall stress lb/in

N_θ = tangential thin wall stress lb/in

ΔP = pressure difference across wall lb/in^2

ϕ = angle between normal to the shell and its axis of revolution

r_2 = length along normal between shell surface and its axis of revolution, in

The resultant situation is an unusual one in that the only principal stress is hoop tension with no stress in the direction of the meridian. This is obviously an oversimplification and probably arises from the assumption here that dF_x is balanced at all stations, while the assumption in the analysis is only that overall ΣdF_x, that is the integrated value, is balanced. Nevertheless, in view of our imperfect knowledge of cavity generator behavior, such simplifications seemed warranted as a means of expediting the analysis.

Next, the relationship for ϕ and r_2 in terms of the parameters of an ellipsoid were combined with Equation (4) to yield a stress equation for any station in the wall of the cavity generator.

$$S_\theta = \frac{\Delta P\, R\left(1 - \frac{X^2}{L^2}\right)}{t\left(1 - \frac{X^2}{L^2}\left(1 - \frac{R^2}{L^2}\right)\right)^{1/2}} \qquad (5)$$

where:

S_θ = tangential stress, lb/in^2

ΔP = pressure drop across wall, lb/in^2

R = base radius of cavity generator, in

t = wall thickness, in

X = axial distance from base, in

L = length of cavity generator, in

The only variable in the right side of this equation which does not depend upon cavity generator dimensions is ΔP, the pressure across the wall at the point of interest. ΔP was calculated from the maximum acceleration, the density of gas at that time, and the density of the liquid.

$$\Delta P = \frac{XA}{g}(\rho_L - \rho_G) \qquad (6)$$

where:

A = maximum acceleration, in/sec^2

g = gravitational constant, in/sec^2

ρ_L = density of liquid propellant, lb/in^3

ρ_G = density of gas at time of A, lb/in^3

This is slightly inaccurate, since it assumes that gas density is linear with distance and hence that the gas is incompressible. However, the gas had already been simplified in other respects in the analysis, and in addition this assumption gives conservative results.

As it turns out, the distribution of stress in the wall of the cavity generator is as shown in Figure 3.2. Stress reaches a peak value at an $\frac{X}{L}$ near 0.7.

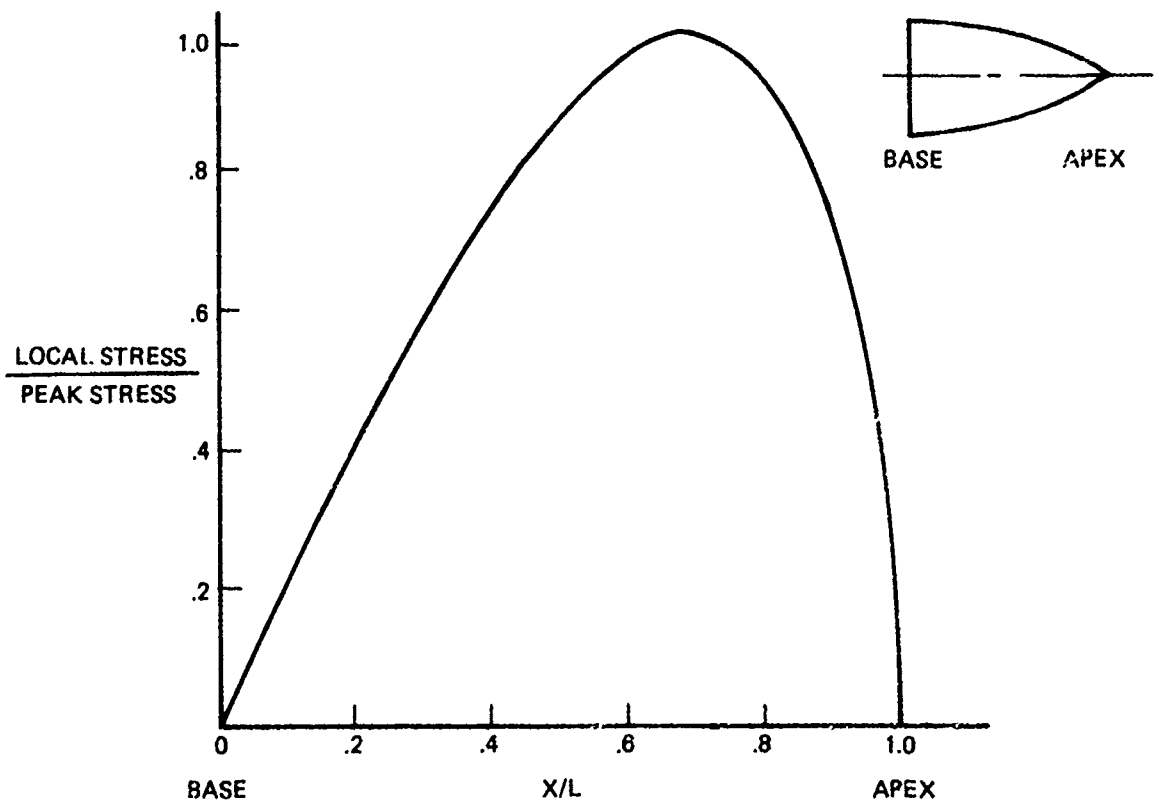

Figure 3.2. Distribution of Stress in Cavity Generator Wall

3.1.1.3 Parametric Study. Now the selection process could begin. We wished to select more than one cavity generator design so that variations in results could be observed. Our intention was to obtain data which would reveal information on performance variability and parametric trends more clearly than would be afforded from a single fixed design. Wide variation in performance within permissible stress levels was the objective.

A computational procedure was pursued as follows: Several values of controlling parameters were selected. A series of computations of dynamic performance were run, and those parameter values for which results were unrealistic were eliminated from consideration. The ranges of parameters for which computations were made are listed in Table 3.1.

Table 3.1

Proj. Wt.	120 gm
C/M	.5, 1.0, 1.5
A1/AC	.8, .6, .4
L	30, 50, 70 millimeters
t	.002 to .020 in .002 increments

where

L = Length of cavity generator
t = Wall thickness

For each set of conditions other than wall thickness, wall thickness was used as the independent variable. Calculation results were scanned, and that wall thickness was selected for which peak stress dropped below 200,000 psi. This is approximately the maximum tensile strength of 13.8 PH Mo stainless steel, condition 1070, being used for the cavity generators. Figure 3.3 shows a typical curve of peak stress as a function of wall thickness for one set of conditions.

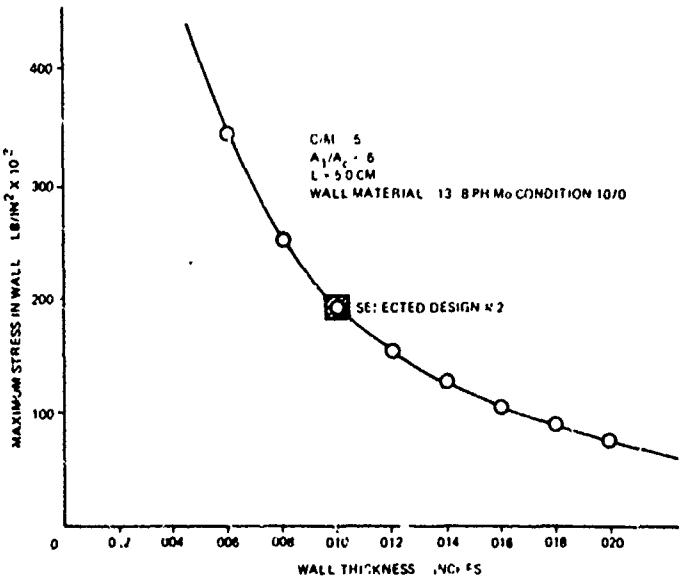

Figure 3.3. Typical Curve of Maximum Stress versus Wall Thickness

The parameters of interest in each instance are muzzle velocity, chamber pressure, and burn-out point. Figure 3.4 shows the results of the screening process. Each point represents the thinnest cavity generator, for parameters as indicated, for which peak stress is below 200,000 psi. Values of peak pressure, cavity generator length, and thickness correspond to each point.

In interpreting these data remember that the computations at this stage were based upon many simplifying assumptions and that trends, rather than particular values, were the information sought. One should not place too much emphasis upon absolute performance numbers.

From this screening three separate designs were selected which should give fairly wide variation in results.

The three cavity generator designs selected are listed in Table 3.2 below.

Table 3.2

Design	Length – mm	A1/AC	Wall Thickness – in
1	50	0.8	0.010
2	50	0.6	0.010
3	50	0.4	0.010

The corresponding points are indicated on the overlay, to Figure 3.4. As can be seen they should permit diverse operating conditions to be observed. For example, the number 1 design should burn-out relatively far down bore. The number 2 and number 3 designs should burn-out nearer the breech and they should allow observation of the effect of A1/AC with C/M held constant. They also will permit investigation of the effect of varying C/M.

3.1.1.4 Circular Arc Ogive Design. In fabricating cavity generators, the shop finds it much easier to work with circular arcs than with ellipsoidal surfaces. A change to a circular arc ogive seemed desirable. A brief study was undertaken to compare shapes comprised of straight segments and circular ogives with the basic ellipsoidal shape. Volume and base area of the ellipsoid were held constant and matched. Straight portions of 0, .1, .2, and .3 of the total ellipse length were used. The .1 shape was found to match the ellipse very closely in the region of highest stress and this was chosen. Figure 3.5 is a diagram showing the geometric comparison between the various shapes and the basic ellipsoid.

It was also necessary to develop new stress equations for the circular ogive configuration and to compare them with those for the ellipsoid. The equation for stress in the cylindrical skirt is that for simple hoop tension.

$$S_\theta = \frac{\Delta P \; R}{t} \qquad (7)$$

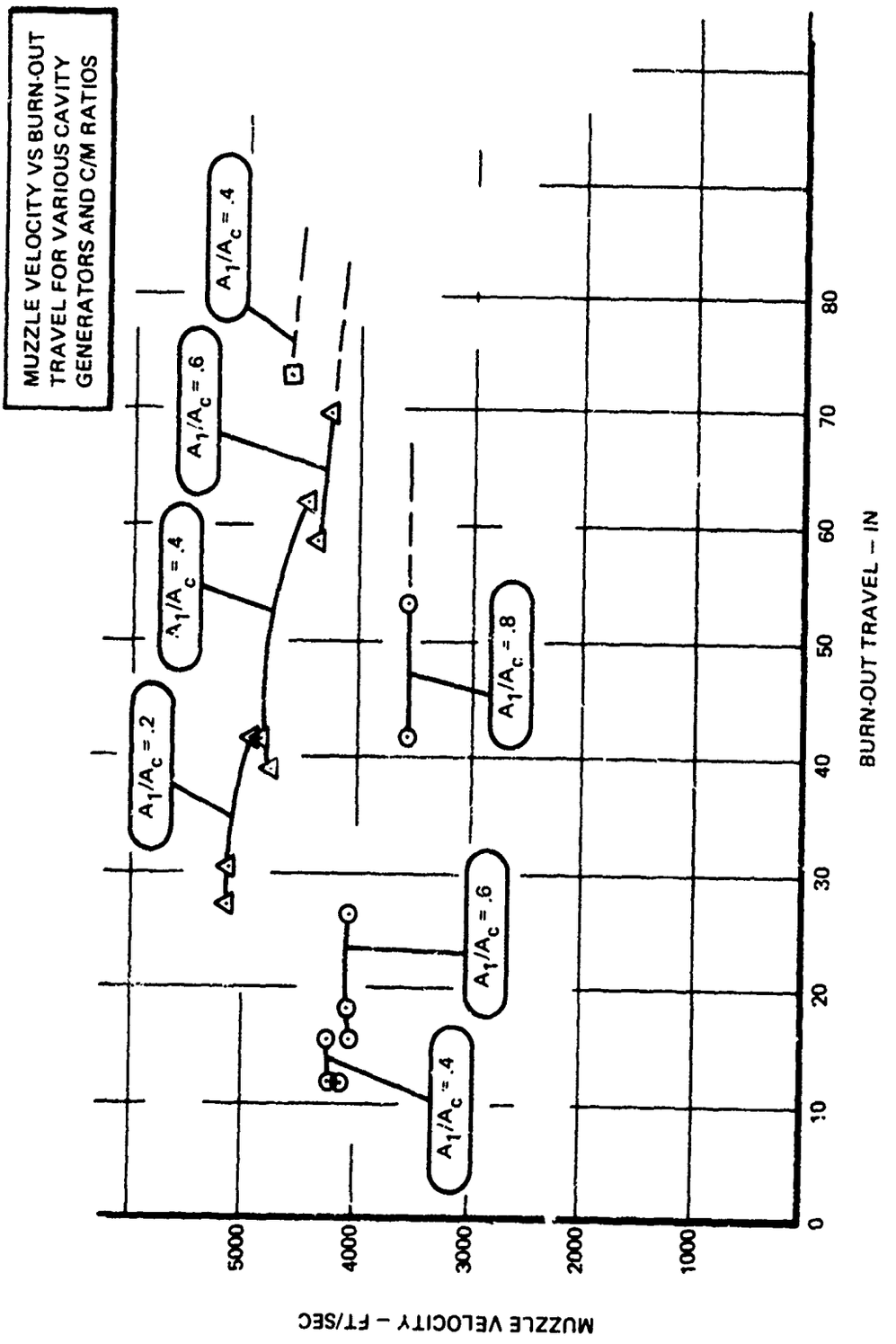

Figure 3.4. Summary of Computation Results

DESIGN #1
DESIGN #3
DESIGN #3

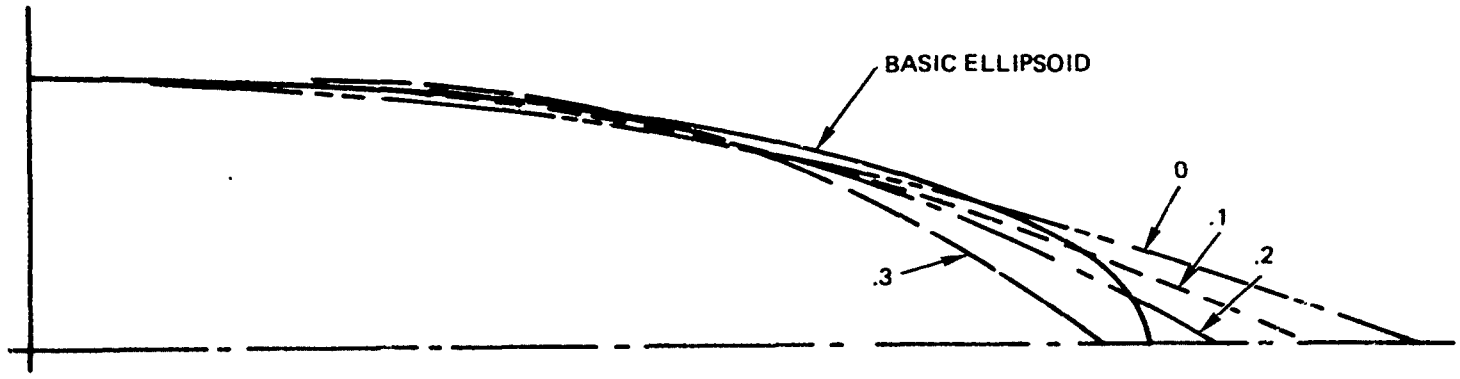

———	ELLIPSE	
— - - - —	0 CYLINDRICAL	R = 12.714
— — — —	.1 CYLINDRICAL	R = 9.245
— — — —	.2 CYLINDRICAL	R = 6.339
— — — —	.3 CYLINDRICAL	R = 3.995

Figure 3.5. Comparison of Cylinder/Circular Ogive Shapes with 2X1 Ellipsoid

Combining the expressions for ϕ and r_2 for a circular arc ogive with equation (4) gives a new expression for wall stress in the ogive portion.

$$S_\theta = \frac{\Delta P}{t}\left(\left(R_C^2 - (X-X_o)^2 - (R_C - R)\,(R_C^2 - (X-X_o)^2)^{1/2}\right)/R_C\right) \qquad (8)$$

where

S_θ	=	tangential stress, lb/in^2
ΔP	=	pressure drop areas wall, lb/in^2
R	=	base radius of cavity generator, in
R_C	=	ogive radius, in
t	=	wall thickness, in
X	=	axial distance from base, in
X_o	=	axial length of cylindrical skirt, in

Comparison was made between the stress distribution for the circular arc ogive, Equations (8) and (6) combined, with that for the ellipsoid, Equations (5) and (6) combined. Figure 3.6 shows comparative plots of stress factor for the three designs. Stress factor is that portion of the equation for local stress which depends upon the physical dimensions of the cavity generator. The graphs show that the change to circular ogives affected the maximum stress very little and, in fact, lowered it slightly.

Figure 3.7 is a sketch of a final cavity generator design.

3.1.1.5 Fabricated Cavity Generators. Four each of the 0.4 and 0.6 area ratios and five of the 0.8 area ratio cavity generators were machined. We intended five of each, but lost two in developing the machining techniques. Figure 3.8 is a photograph of three machined cavity generators, showing the three different sizes.

The completed cavity generators were weighed and compared with the theoretical weights. Results are shown graphically in Figure 3.9. They tend to be slightly heavier than theoretical, but the difference amounts to an average wall thickness difference of only 0.005 inch for the largest deviation and less than 0.002 inch for most of the rest. This seemed perfectly adequate. Later on, when more was known about the configurations desired, more accurate tooling methods could have been devised. Meanwhile, we demonstrated that test items could be conveniently machined from PH13-8 Mo stainless steel.

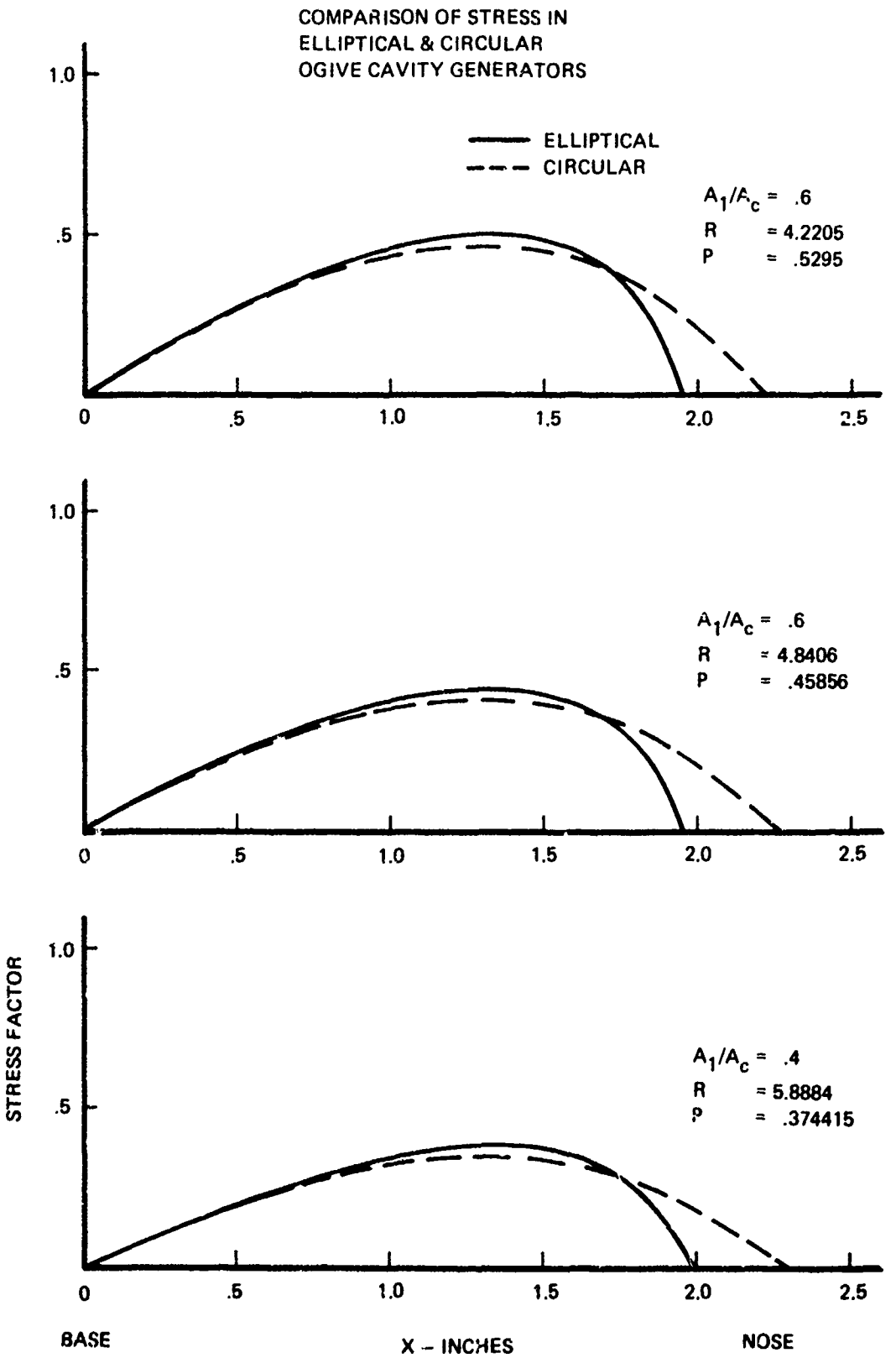

Figure 3.6. Comparison of Stress in Elliptical and Circular Ogive Cavity Generator

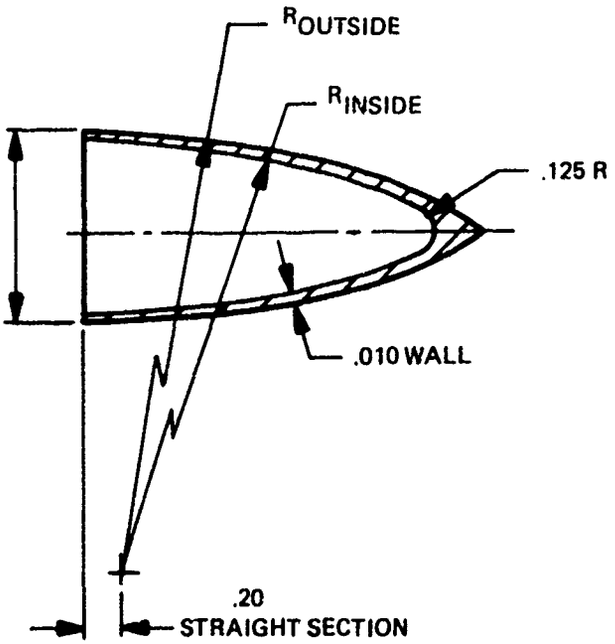

PART	D	$R_{OUTSIDE}$	R_{INSIDE}
–1	1.060	4.220	4.210
–2	.920	4.840	4.830
–3	.750	5.880	5.880

DIMENSIONS IN INCHES

MATERIAL: PH 13–8 Mo STAINLESS STEEL
CONDITION 1070

Figure 3.7. Hollow Shell Cavity Generator Design

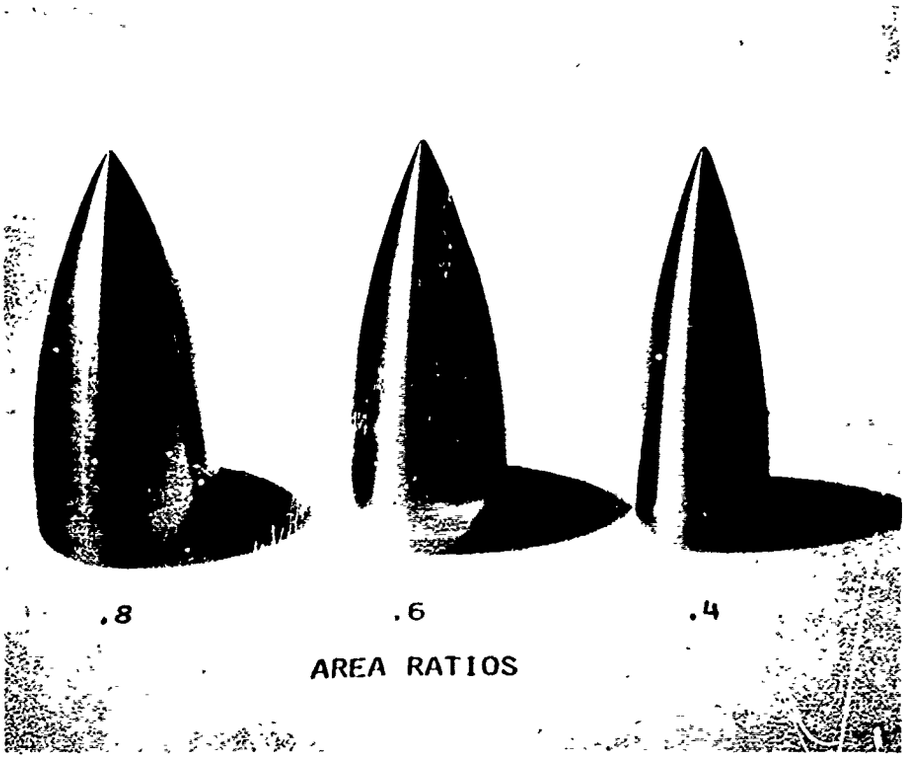

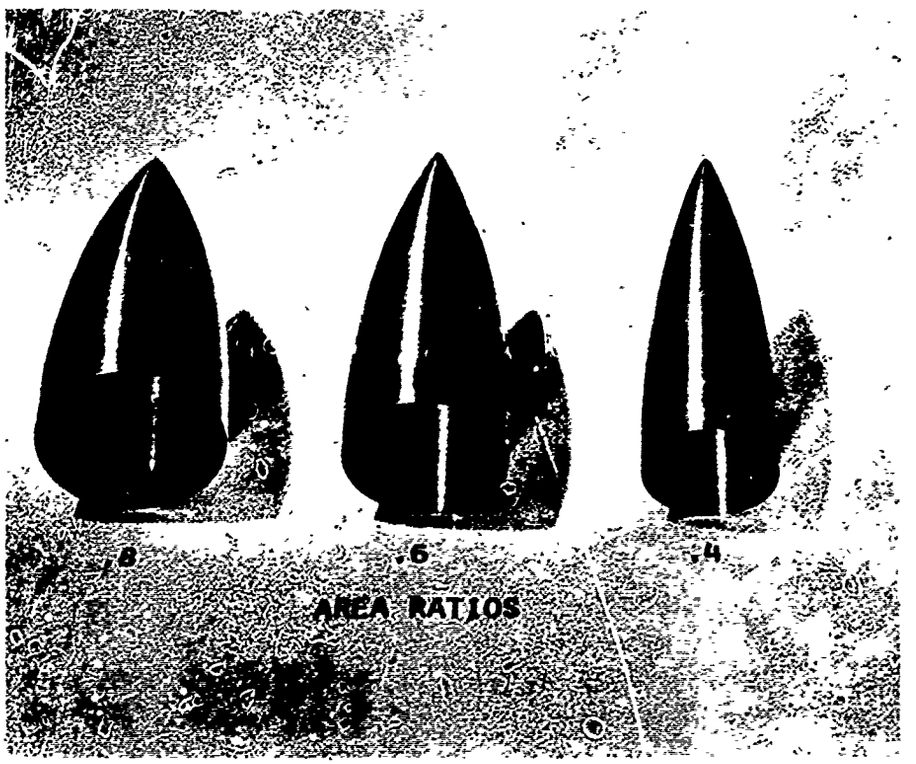

Figure 3.8. Machined Hollow Shell Cavity Generators

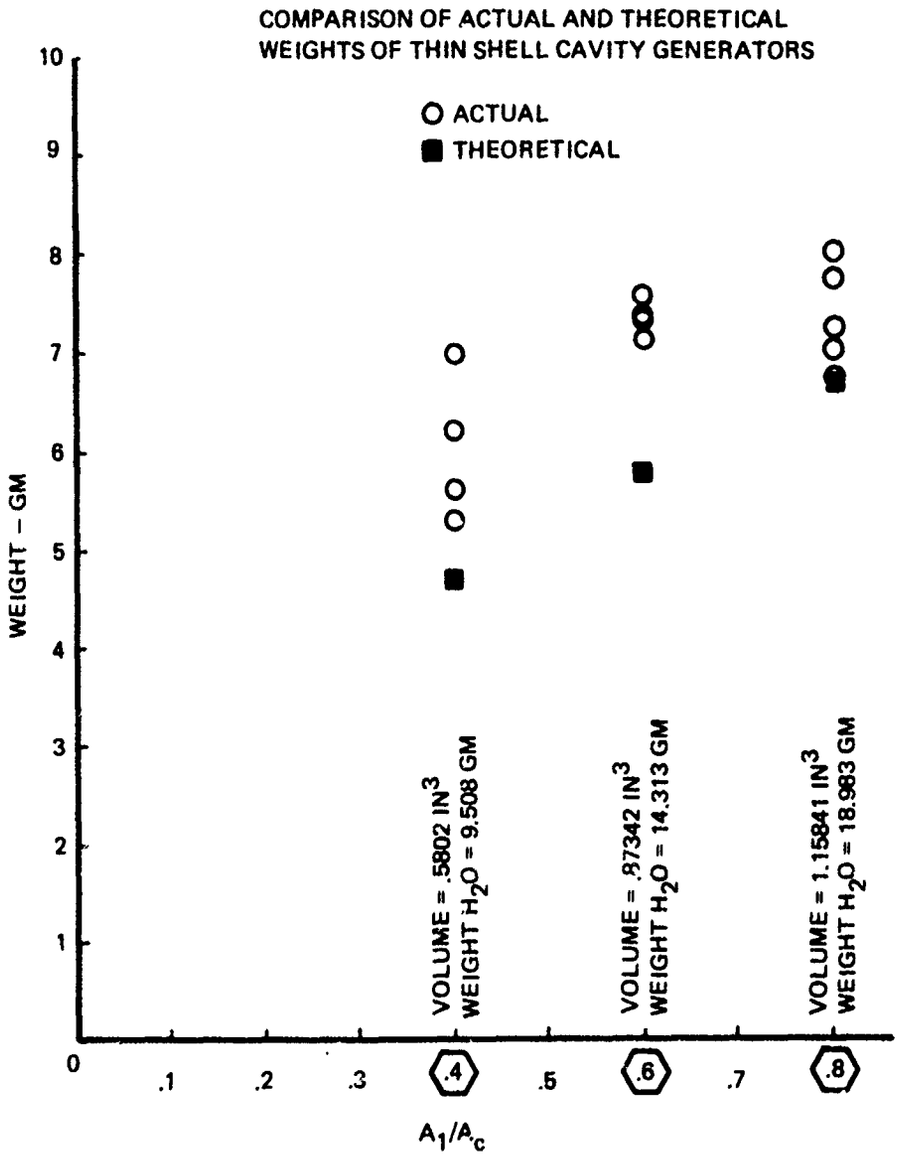

Figure 3.9. Comparison of Actual and Theoretical Weights of Thin Shell Cavity Generators

3.1.2 MULTIPLE-HOLE CAVITY GENERATOR DESIGN

3.1.2.1 Basic Concept. Section 3.2 will explain how the hollow shell cavity generator proved unsuccessful. The first firing tests suggested an insufficient liquid/gas interface. Presumably, a larger liquid surface area would be required for more desirable burning characteristics.

At this stage in the program, we assumed that the shape of the cavity generator controls the liquid/gas interface. In our concept model, liquid flowing relatively rearward leaves the cavity generator in a cylindrical sheath whose contour is controlled by the shape of the cavity generator cross-section. If our model was correct, the easiest way to increase the liquid surface would be to change the shape of the cavity generator. Specifically, the new cross-section should have a greater total surface length. The problem reduces to searching for geometrical cross-sections which have increased lengths of perimeter for a given enclosed area. Figure 3.10 illustrates a number of possibilities considered.

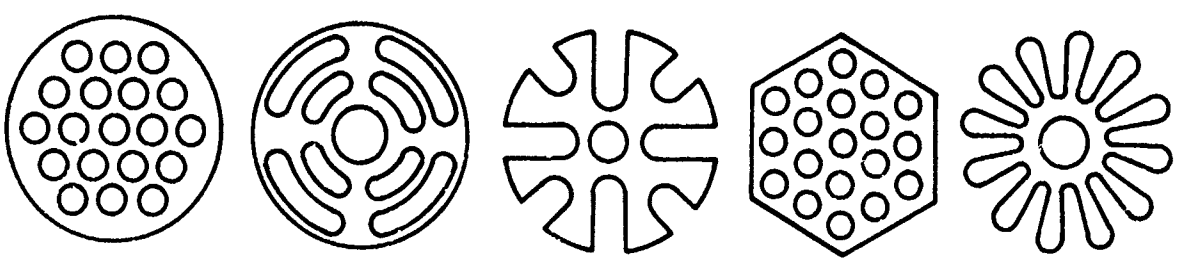

Figure 3.10. Possible New Cross Sections

Cavity generators constructed with any of the cross-sections shown should generate liquid/gas interfaces with much more area than does the purely circular cross-section.

3.1.2.2 Practical Considerations. While any of the shapes shown might achieve the desired results, the practical aspects of fabrication had to be addressed. None of the shapes shown appear easy to fabricate as thin steel shells. Sophisticated tooling would be required for any of them. A decision was made to make them solid from low density materials.

The requirement remained, however, that density of the cavity generator displacement body must be less than that of the liquid propellant. Lightweight plastics seemed appropriate as candidate materials.

The question of material strength immediately arose. Plastics are not notable for high strength. On the other hand, the primary mode of loading to which the cavity generator is subject is pure hydrostatic compression. Data are not readily available on the strength of plastics under isostatic pressure loading. We guessed that conventional data on tensile and compressive strengths are based upon uniaxial loading and do not really apply here. We decided to emphasize density considerations and to observe in tests what happened with regard to material strength properties. Table 3.3 lists several plastics

Table 3.3

Candidate Plastics for Multiple Hole Cavity Generators

Material	Specific Gravity	Tens. Str KPSI	Compr. Str KPSI
ABS	1.01-1.06	4.5-6.0	–
Nylon 12	1.01	7.1-8.5	–
Nylon 6/12	1.06-1.08	8,8	2.4
Phenylene Oxide (Noryl)	1.10	7.8	12
Polybutylene	894-.91	.9-2.2	–
Polymethyl Pentene	.83	4	–
Polyethylene			
Low Dens	.91-.925	14-2	–
Med Dens	.93	2.3-2.4	–
High MW	.94	5.4	
Propylene-Ethylene	.91	4	
Polypropylene	.9-.91	4.9-5.2	5.5-6.5
Polystyrene	1.04	5-10	11.5-16

Polypropylene was selected as having the best balance of low-density and high tensile and compressive strengths.

Fabricating techniques further influenced our design. Complicated shapes suggest awkward machining requirements. On the other hand, cylindrical surfaces can be turned, round holes can be drilled, and flat surfaces can be milled. A combination of these types of surfaces seemed the most practical. The choice thus quickly focused on round or hexagonal multiple hole shapes.

3.1.2.3 Fabricated Cavity Generators. In all, four different cross-sections, two different lengths, and two types of holes were represented in the cavity generator designs fabricated and tested. In addition to geometrical difference between those selected, features allowing three different methods of mounting or securing in firing position were tried. Table 3.4 summarizes the various types and arrangements.

Table 3.4

Multiple Hole Cavity Generators

1.	19-hole circular. Fired at C/M = .5.	No skirt.	1-inch long.	
2.	19-hole circular. C/M = .75, and 1.0.	Attached skirt.	1-inch long.	
3.	19-hole circular. C/M = .75.	Separate skirt.	1-inch long.	
4.	36-hole circular. C/M = .75.	Separate skirt.	1-inch long.	
5.	19-hole circular. C/M = .75.	Separate skirt.	2-inches long.	
6.	19-hole hexagonal. C/M = .75.	Straight holes.	Separate skirt.	1-inch long.
7.	19-hole hexagonal. C/M = .75.	Tapered holes.	Separate skirt.	1.375 inch long.

Basically, each cavity generator was a solid polypropylene plug through which longitudinal holes were drilled. For all cavity generators, the ratio of base area to total bore area was maintained at 0.6. This was the intermediate value for the hollow steel cavity generators. As Table 3.3 indicates, the specific gravity of polypropylene is 0.9.

Figures 3.11, 3.12, and 3.13, show several of the multiple holed cavity generators which were fabricated.

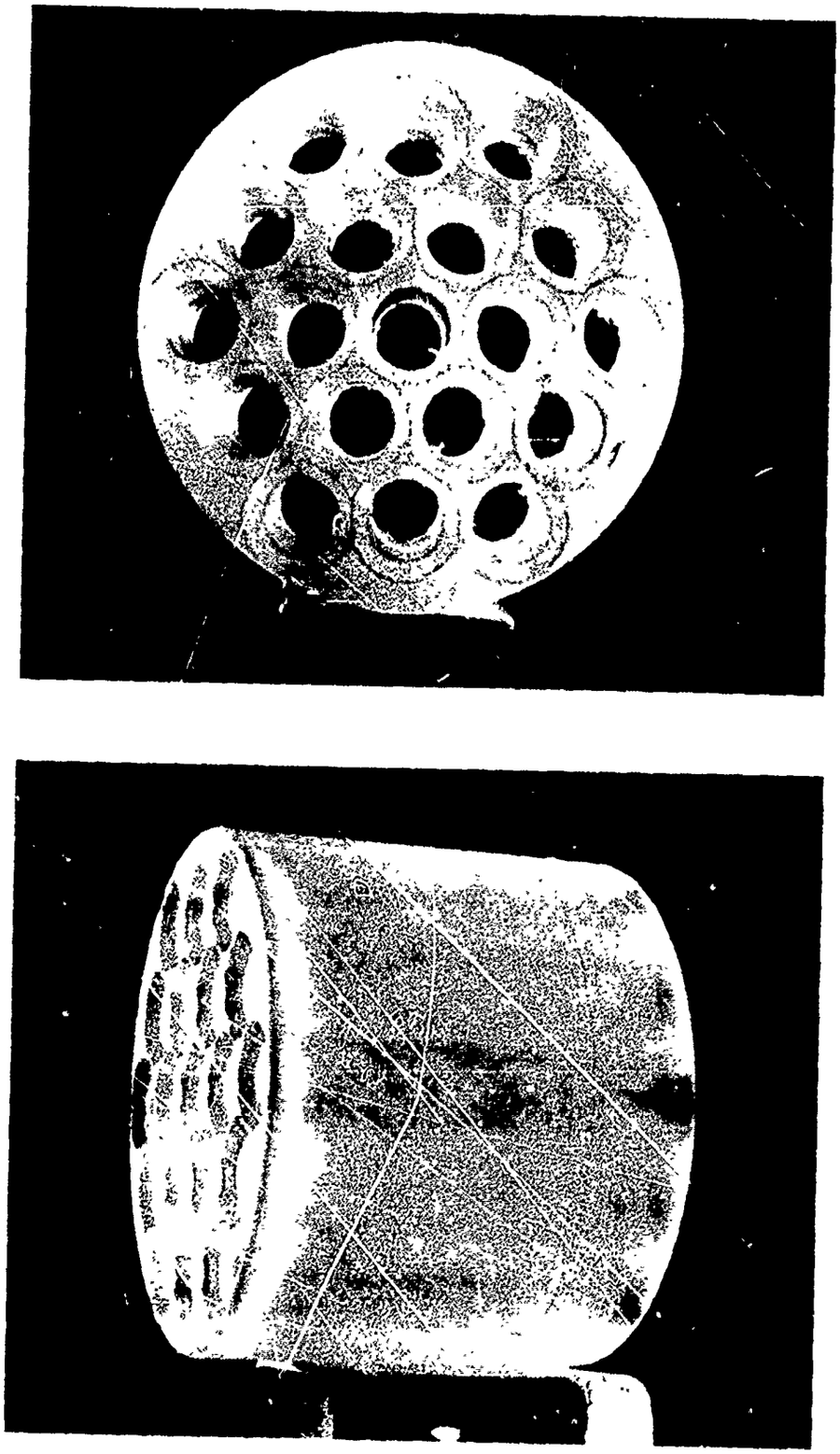

Figure 3.11. Original 19-Hole Polypropylene Cavity Generator

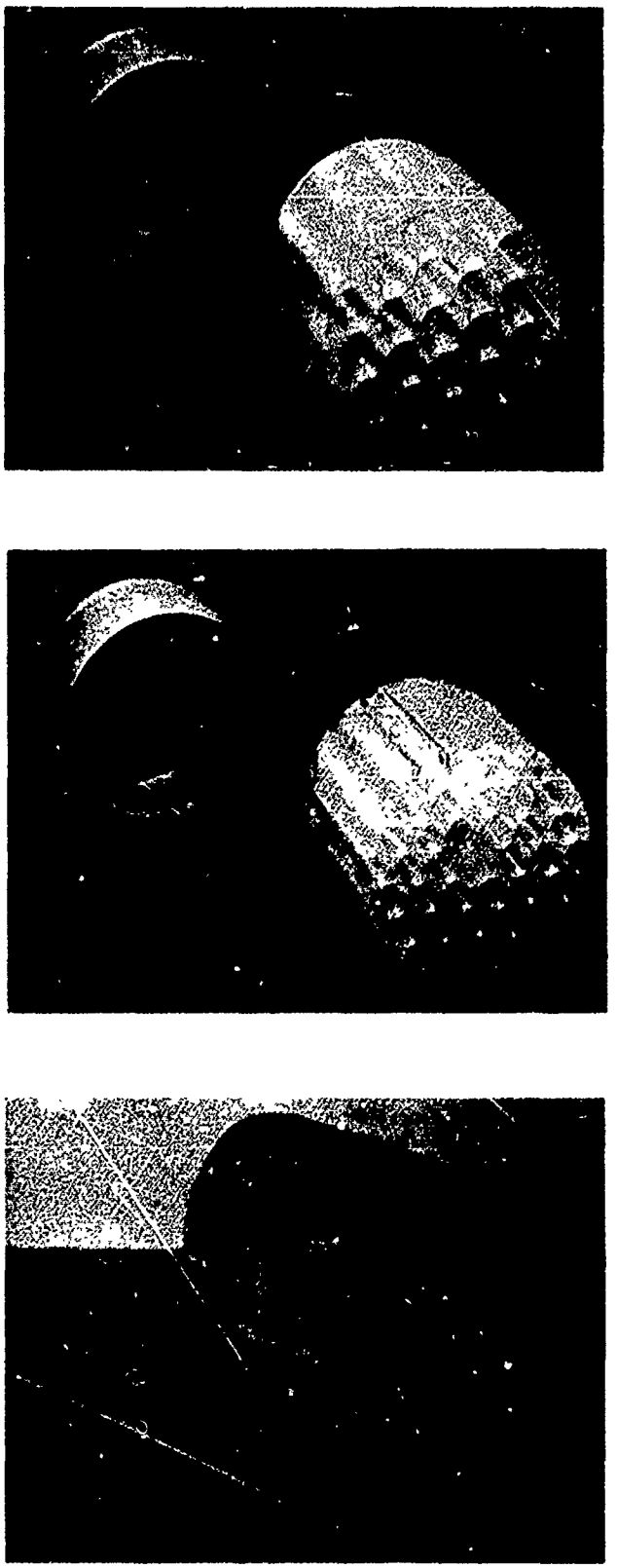

Figure 3.12. 19-Hole and 32-Hole Designs with Separate Skirts

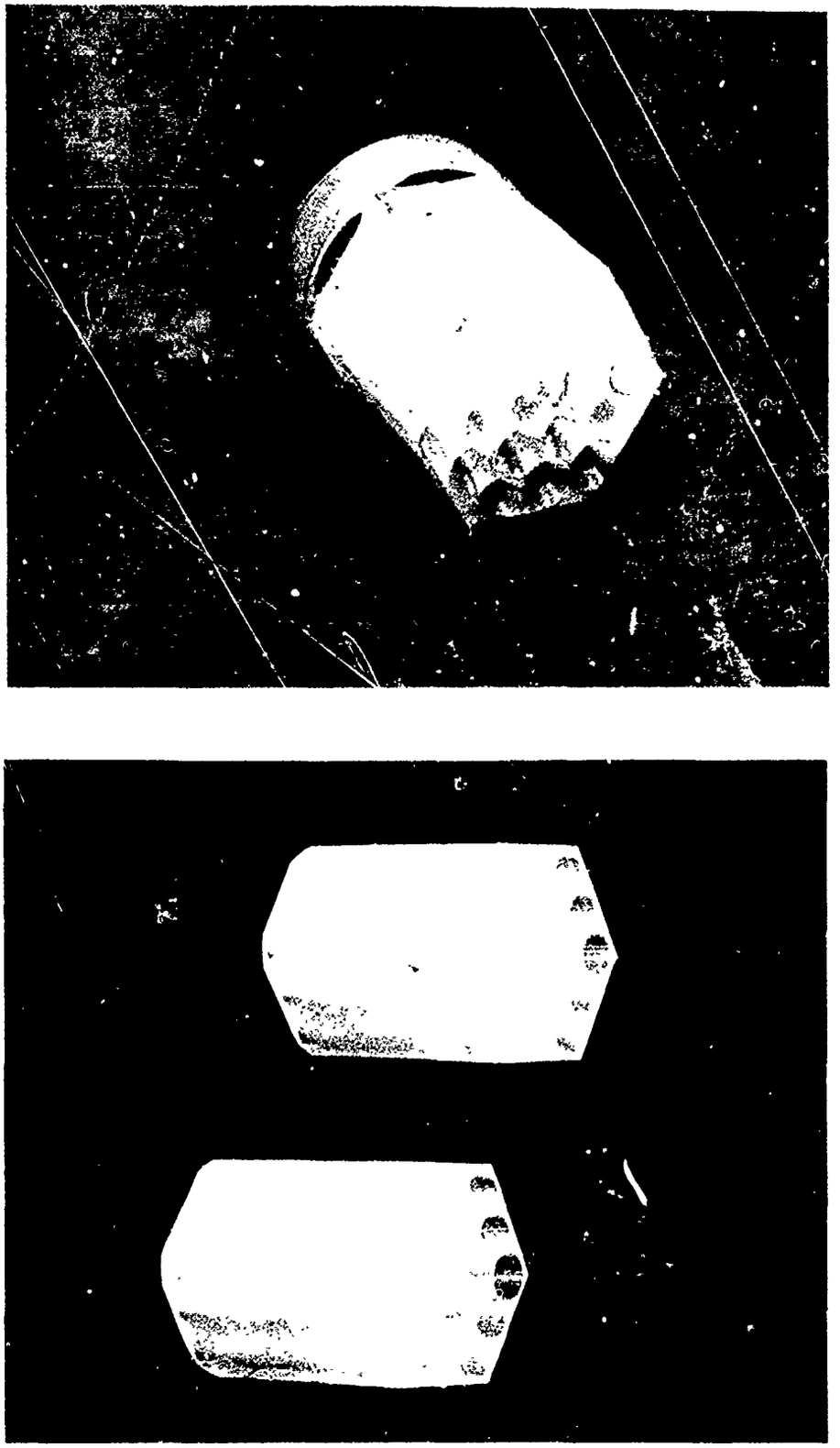

Figure 3 13. Hexagonal Designs

3.2 Task 2 – Single Shot Firing Tests

3.2.1 TEST FIXTURE DESIGN

3.2.1.1 General Arrangement. The design of the test fixture is simple and straightforward. Simplicity was stressed to assure that test setup and fixture maintenance required a minimum of time and emphasis. Technicians could thus concentrate on firing procedures and instrumentation, which are critical elements in achieving accurate results. A design was developed for which propellant can be loaded into the chamber and, if desired, downloaded from a control position outside the test bay. Firing is controlled from the same position, of course. Figure 3.14 is a diagram of the test fixture showing the general arrangement. The smooth-bore 30mm barrel is secured in clamps which are in turn mounted resiliently to a structural I-beam. A threaded breech plug supports the firing load. Fill and drain valves are located at the top and bottom of the chamber. A pressure transducer is provided for measuring chamber pressure near the breech. Position sensors are provided at three stations down-bore. At each station, both light-beam and pressure sensing is provided.

3.2.1.2 Details of Breech Design. Figure 3.15 shows the general details of the breech design with a cavity generator, liquid charge, and projectile in position for firing. M52 electric primer is used for initiating the ignition process. A booster charge forward of the primer ignites the main propellant charge. The type of booster charge and its arrangement changed as the program proceeded and also varied with the type of cavity generator used.

3.2.1.2.1 Design for Hollow Shell Cavity Generators. The hollow shell cavity generators were originally retained in cylindrical bores in the primer support. A booster charge of Hercules Bullseye solid propellant was placed inside. The need for the booster charge was indicated by two tests in which primers alone were fired into a volume equivalent to the largest cavity generator. Approximately 1000 PSI was generated. We felt this reflected insufficient energy to generate burning in the main charge.

The length of the bore in the primer support was arbitrarily selected as 0.6 inch. Thus, the cavity generator had to move 0.6 inch within the primer support before exiting and exposing propellant to the booster gases.

A technique for sealing and securing the cavity generator in the primer support was devised. Epoxy cement applied at the base skirt of the cavity generator as it rests in the primer support provided a vacuum-type seal and had sufficient strength to secure the cavity generator against the one atmosphere pressure differential which might exist during loading.

A small test fixture was used to check the effectiveness of the seal. The cavity generator and the primer support could be placed at the bottom of a column of water and the space above the water could be evacuated. Any leakage showed as air bubbles leaking past the seal up the water column.

The tension force was checked by applying pressure through the priming hole until the epoxy joint sheared. A pressure of over 100 PSI was necessary to shear the largest diameter cavity generator from the support.

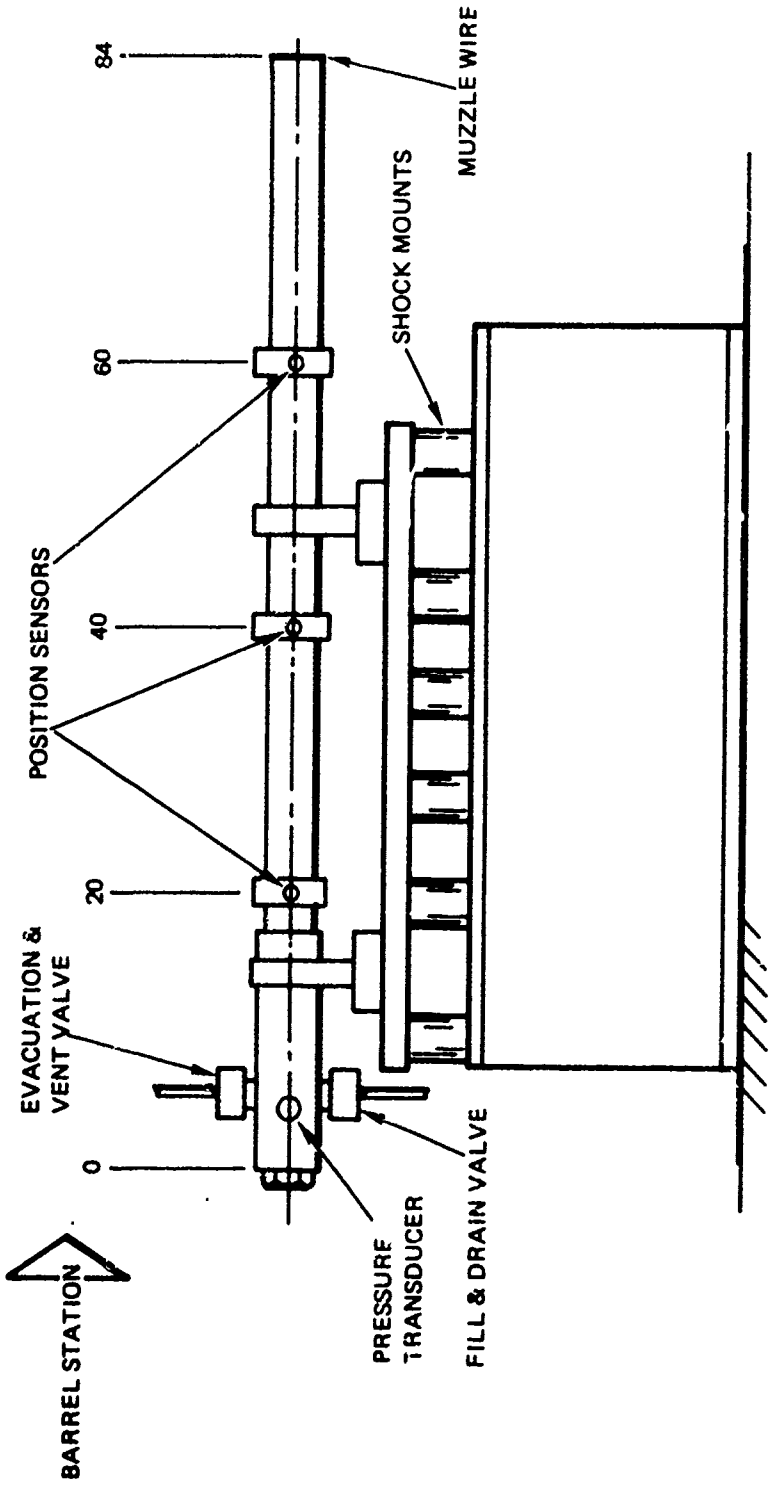

Figure 3.14. General Arrangement of Test Fixture

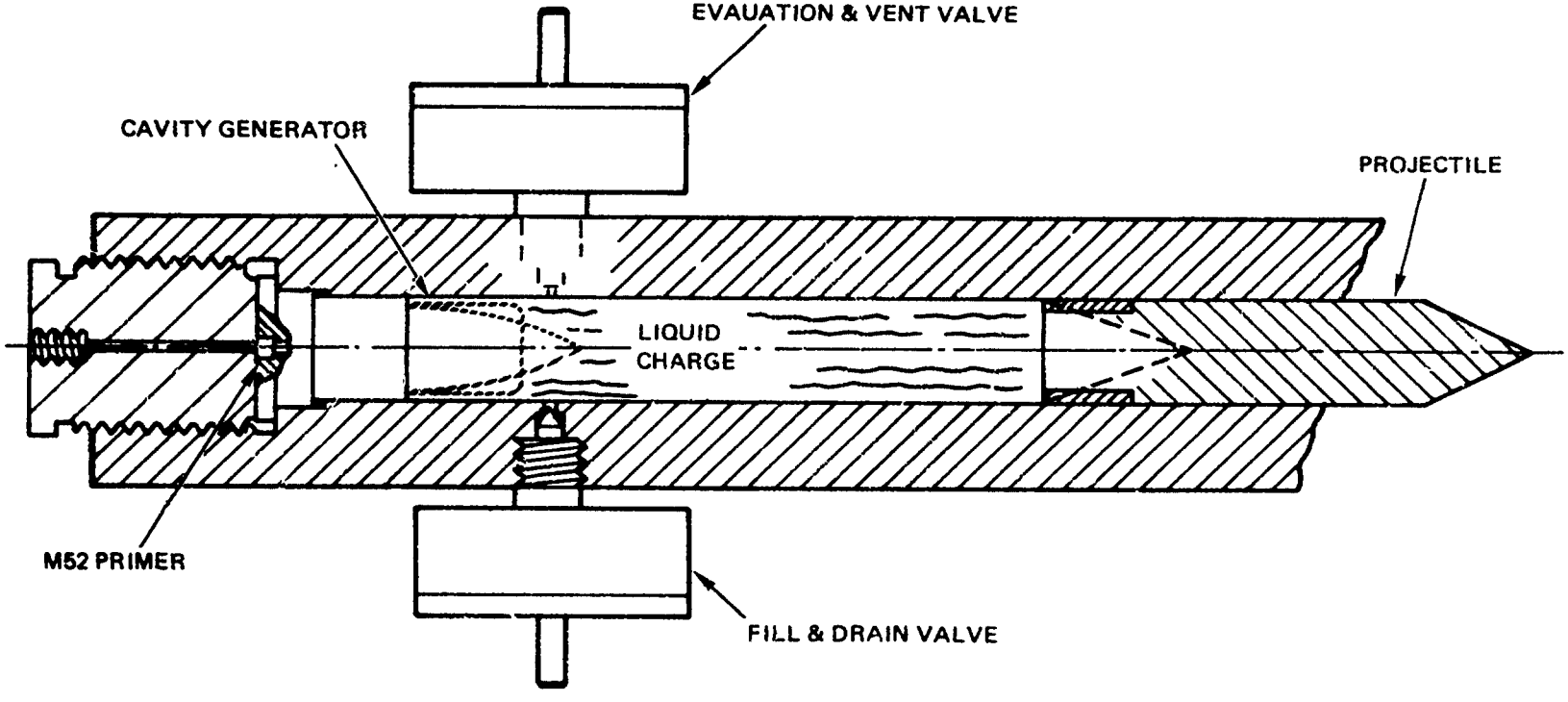

Figure 3.15. Test Fixture Breech Design

Figure 3.16 shows the firing configuration. Care was taken in loading the Bullseye booster charge to place it in the nose of the cavity generator. When the cavity generator was loaded in the horizontal position shown, the charge undoubtedly slumped down toward the bottom, but we assumed that it remained generally in the forward part of the cavity generator. Since three different cavity generators were used in the tests, separate primer supports were machined, one for each diameter.

A change in priming system was made when the Bullseye solid propellant booster charges did not prove successful. This matter is discussed in Section 3.2.7. Figure 3.17 illustrates the second arrangement.

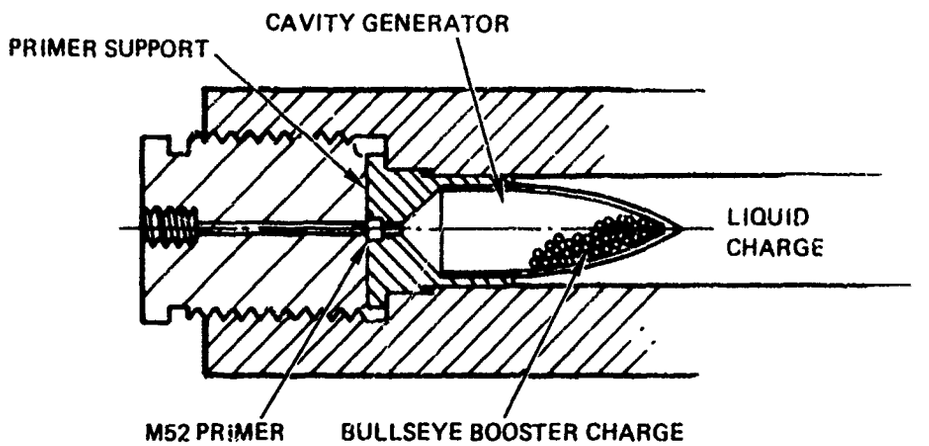

Figure 3.16. Initial Firing Configuration - Hollow Shell Cavity Generator

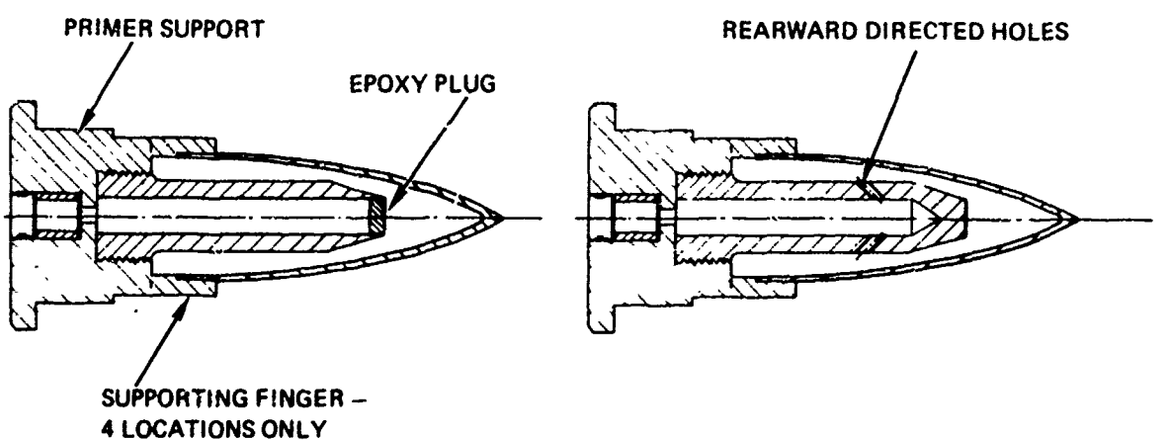

Figure 3.17. NOS 365 Ignition Configurations – Hollow Shell Cavity Generator

A small pre-combustion chamber is located directly ahead of the primer. This in turn leads to a larger booster volume – 0.25 inch in diameter and 2.25 inches long, closed at the forward end with a frangible plug. Epoxy cement was found to work well as a plug. NOS365 propellant was placed in both cavities. The smaller cavity held 0.14cc of propellant, and any additional quantity used in the firing was placed in the larger volume. Charges could be conveniently varied. The cavity generator was immersed in the main charge and, therefore, had propellant within its cavity. Figure 3.18 shows photographs of components of this type of primer support with a cavity generator.

Two further variations of this arrangement were used in the test program. One was a small plug of styrofoam placed in the nose of the cavity generator. This displaced fluid and reduced the quantity of charge in that region. The second variation was the introduction of some rearwardly directed holes in the cylindrical portion of the booster tube in place of the single hole at the front. Figure 3.17 shows the rearward pointing hole arrangement.

3.2.1.2.2 Design for Multiple Hole Cavity Generators. The breech design for firing the multiple hole cavity generators provided a 5.1cc volume behind the cavity generator in which energizing gas could initiate the firing action. Before firing, this volume was isolated from the liquid charge by a thin polyethylene membrane stretched across the back face of the cavity generator and by appropriate seals around the periphery.

Energizing gas was generated in a booster cavity similar in design to the second design used with hollow shell cavity generators. The primer fired through a small pre-combustion chamber full of propellant into a larger chamber. Additional propellant at somewhat lower loading density was in the second chamber. Gases left the booster chamber through six radial holes and entered the energizing volume behind the cavity generator. The jets were directed radially to avoid direct impingement of the hot gases against localized areas of the rear face of the cavity generator.

At first, the cavity generator was simply sealed with the polyethylene sheet, loaded, and placed ahead of the primer support. Silicone grease sealed the periphery. This arrangement proved an awkward one to load, and a skirt was next added to the primer support to secure the cavity generator to the primer support before firing. Figure 3.19 shows this version of the primer support together with a projectile and a cavity generator. The radial booster holes are visible in the central hex of the primer support. The steel skirt expanded on the first firing and made the primer support difficult to remove. The steel skirt was eliminated and a plastic skirt was added to the cavity generator. This skirt snapped over a recess machined on the primer support. Later, a separate skirt was used. Figure 3.20 illustrates the final breech design used for firing the multiple hole cavity generators.

3.2.1.3 Inertial Shot Start. A shot start shoulder was not provided in the present design. We planned to fire with varying charges and with different cavity generators. Projectile position would not be constant for all tests. Fixture design was much simplified if we did not have to provide a shoulder at each different position. We relied on a tight initial fit to hold starting position and on inertia effects thereafter in initiating the combustion process. We felt that if early testing indicated that a step shoulder was necessary, one could be added. None proved necessary, at least in initiating ignition. Whether performance would have been noticeably different with shot start is not yet known.

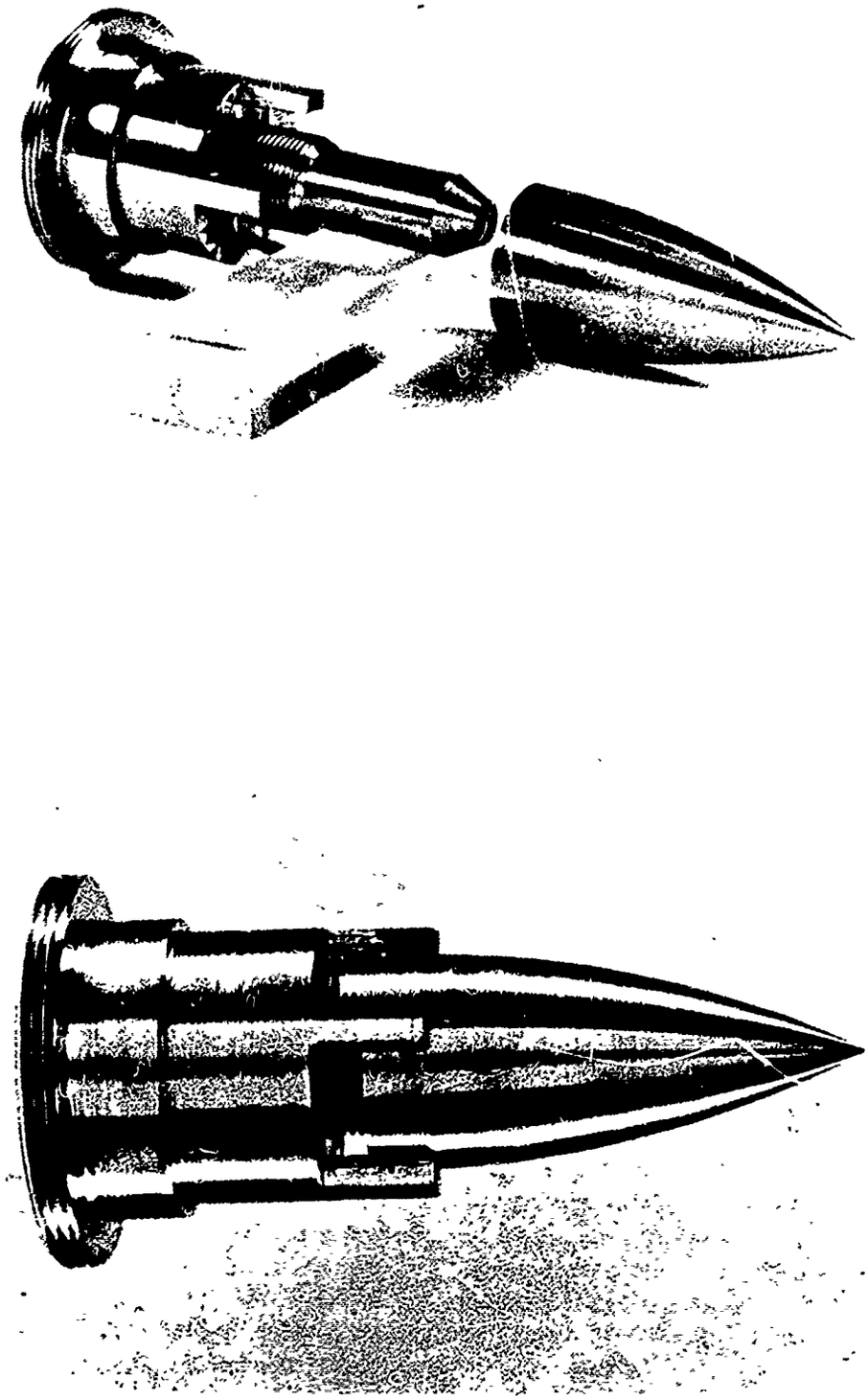

Figure 3.18. NOS 365 Ignition System Components

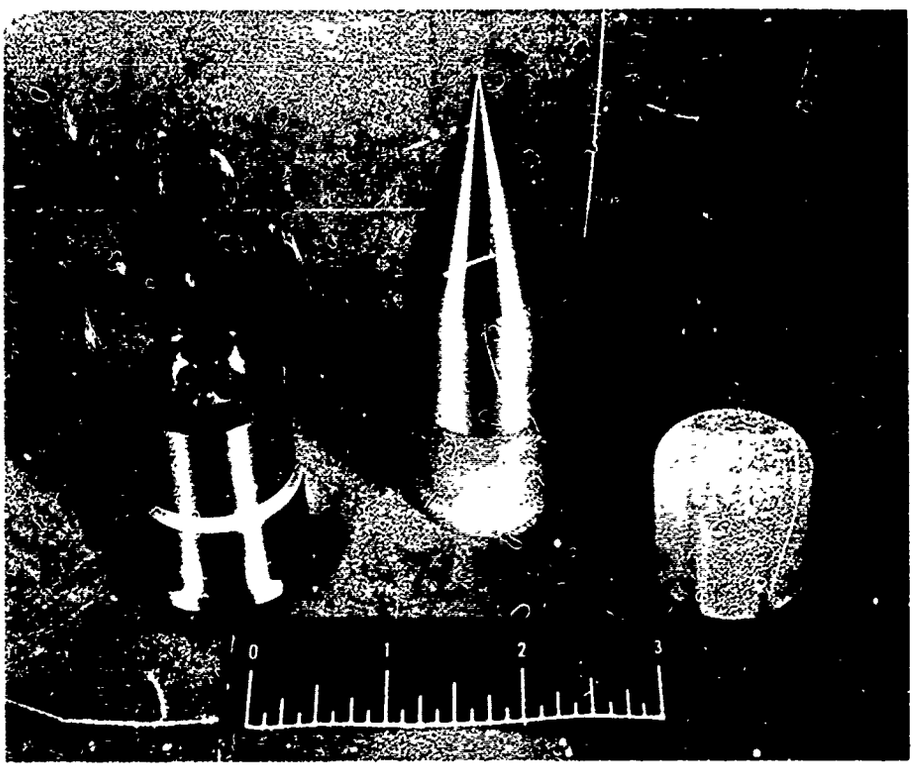

Figure 3.19. Components for First Multiple Hole Cavity Generator Firing

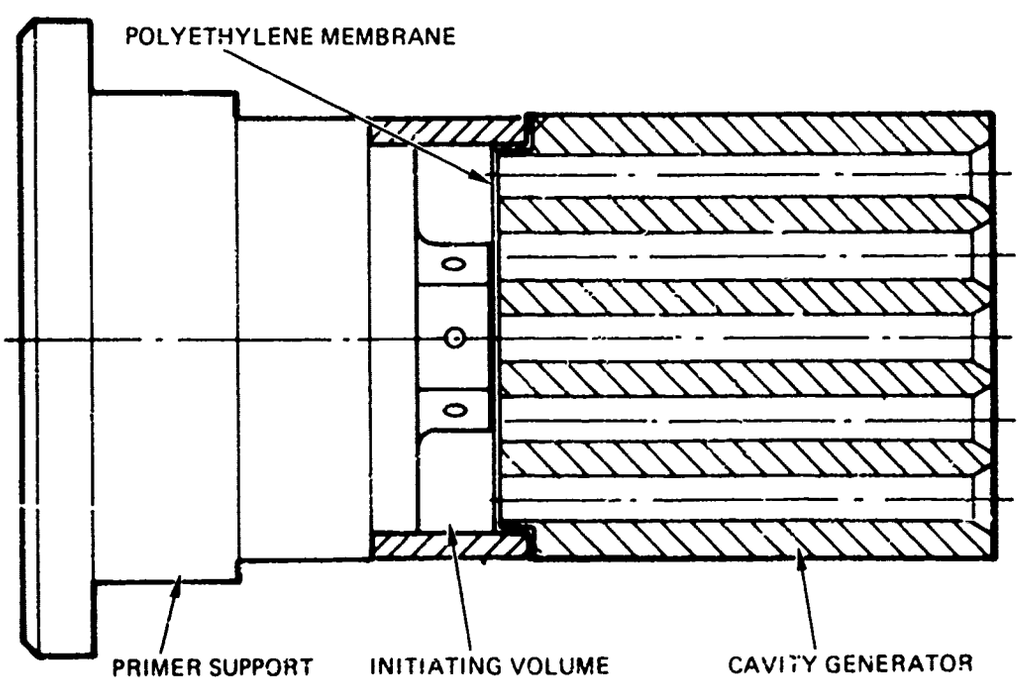

Figure 3.20. Final Breech Design – Multiple Hole Cavity Generators

3.2.1.4 Fill and Vent Valve Design. Identical fill and drain valves were used at the top and bottom of the chamber. The valve at the top served as a vent and evacuation port, and the valve at the bottom was used to load and, if desired, drain the propellant charge. The valves are simple pressure operated needle valves. Figure 3.21 is a cross-sectional view showing details of valve construction. A hole runs most of the length of the needle stem but is offset near the sealing end. The stem also incorporates a piston disk. Gas pressure acting on the piston disk can be used to seat or lift the needle. When pressure is applied to seat the needle, a seal is affected at the 1/16 chamber hole. The ratio of piston area to sealed area is approximately 1000/1, so a modest gas pressure can balance typical chamber pressures. Pressure applied to lift the needle from its seat will open a flow path from the chamber through the offset stem hole and on up the center of the stem.

3.2.1.5 Light Beam Sensor Installation. Figure 3.22 shows details of the light beam position sensor installations. A plexiglass window is secured ahead of one element of a subminiature light emitting diode through-bore pair, either emitter or detector. Its companion is mounted opposite. In this way, a light beam is established across the bore. Passage of any solid body past the sensor interrupts the beam. A bright flash of burning gas appears brighter than the light emitting diode so is also detectable. While we had originally hoped to be able to distinguish unburned propellant passing the station, tests showed that liquid appeared opaque to the sensors.

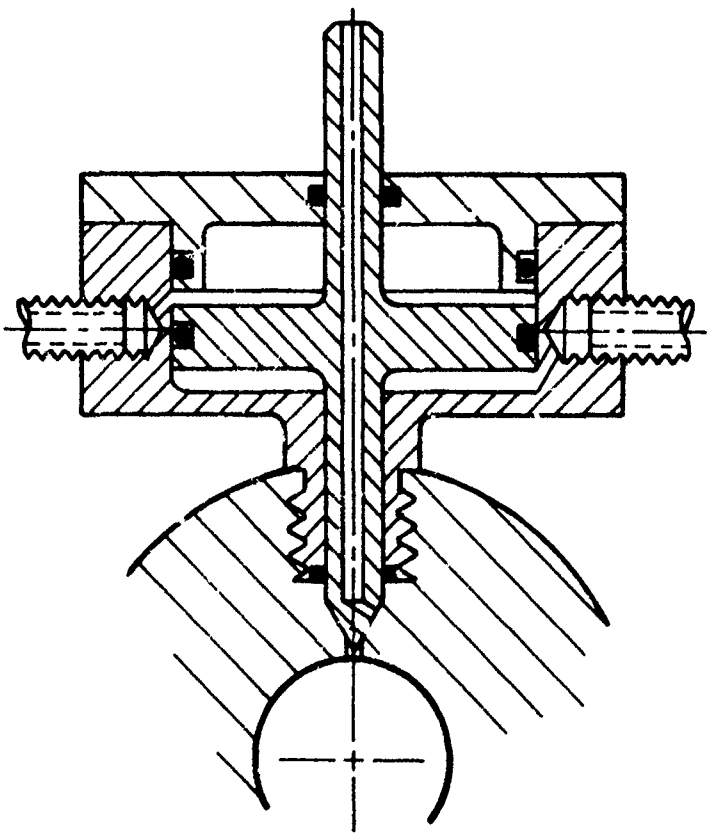

Figure 3.21. Propellant Loading Needle Valve

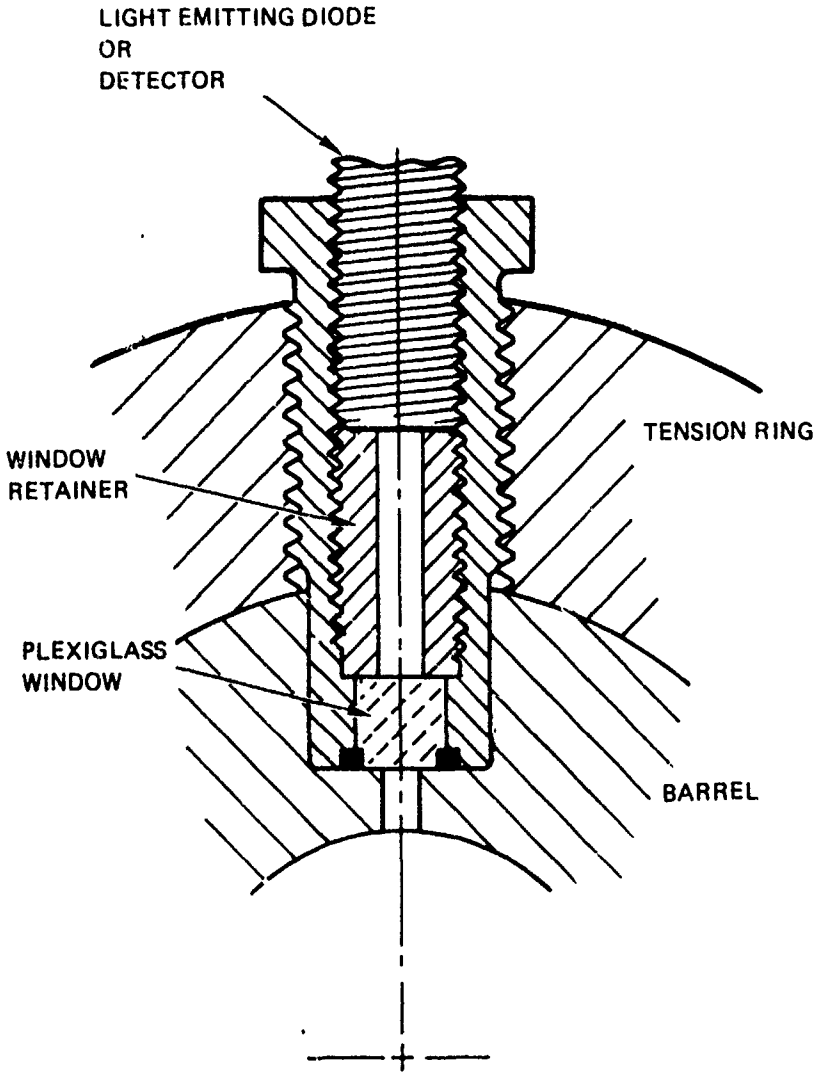

Figure 3.22. Position Sensor Assembly

3.2.2 Propellant Loading. The propellant supply system schematic is shown in Figure 3.23. Loading was accomplished by first filling the lines as far as the left hand drain valve, which is a hand operated ball valve. The fill valve was then closed, and the left hand drain valve opened to permit fluid to flow up toward the fill valve. The firing lane doors were closed and action thereafter was controlled remotely. The vent and fill valves were opened. Propellant flowed into the chamber under the action of gravity until it began to rise in the vent tube above the chamber. The fill valve was closed. By starting the vacuum pump and by sequentially operating fill and vent valves, any bubbles trapped in the chamber were gradually worked out until no ullage remained. Both vent valve and fill valve were then closed for firing. In the event of misfire or the desire to drain the system for any other reason, the power operated drain valve shown at the lower right in Figure 3.23 could be remotely operated. Opening vent and fill valves then permitted the propellant to drain out. The water flush could then be turned on to flood the chamber.

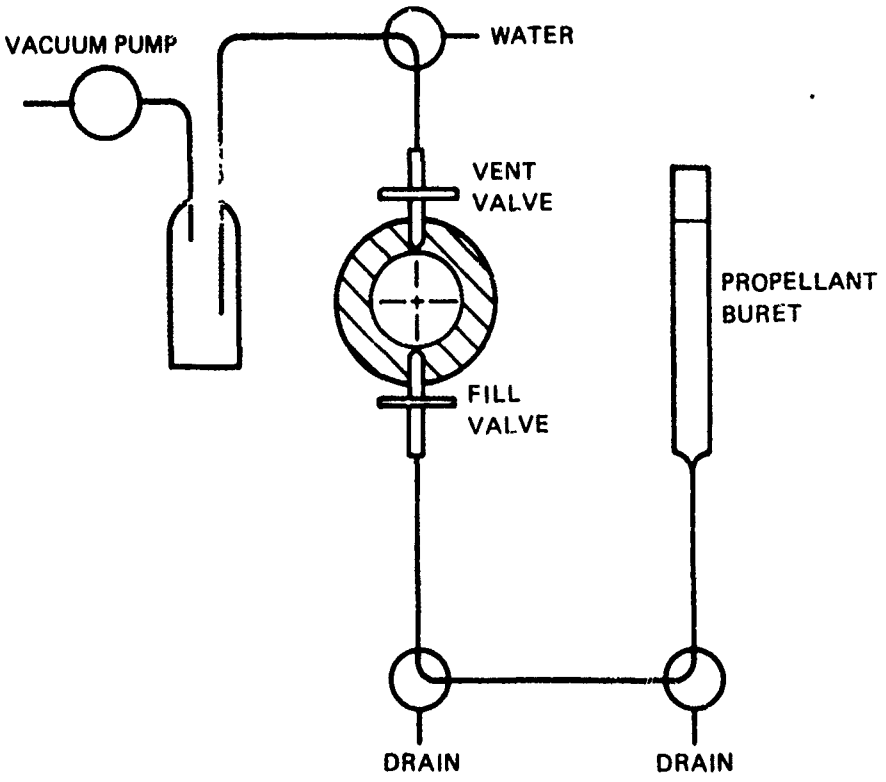

Figure 3.23. Propellant Supply System Schematic

After the first four shots, the vacuum sequence was eliminated. Projectile position was maintained only by tightness of fit, and this was difficult to maintain constant from shot to shot. Occasionally the projectile moved when the chamber was evacuated.

With the vacuum eliminated, gravity fill was used to load the chamber. The flow was sufficiently slow to allow almost all trapped air to leave the vent valve as the fluid entered.

3.2.3 Test Fixture Assembly and Checkout. When fabrication of components was complete, the test fixture was assembled on the I-beam base. The propellant buret was mounted above the test fixture in a bracket attached to the I-beam. Propellant line routing was arranged, and valves were mounted. Figure 3.24 is the basic test fixture in the assembly area before installation of instrumentation or pneumatic control lines.

A control console was assembled and wired. The console enables fill, vent, drain and flush valves to be operated remotely from outside the test cell.

The test fixture was checked out before being moved into the test cell. Control functions were verified by running through filling, firing and draining simulations using water to simulate propellant. A Plexiglass chamber was built for this purpose. This chamber simulated the breech area of the actual barrel. Using the chamber, we were able to observe the filling and draining processes. Figure 3.25 is a photograph of the transparent chamber installed in the test fixture, with a projectile, primer support, and cavity generator in position.

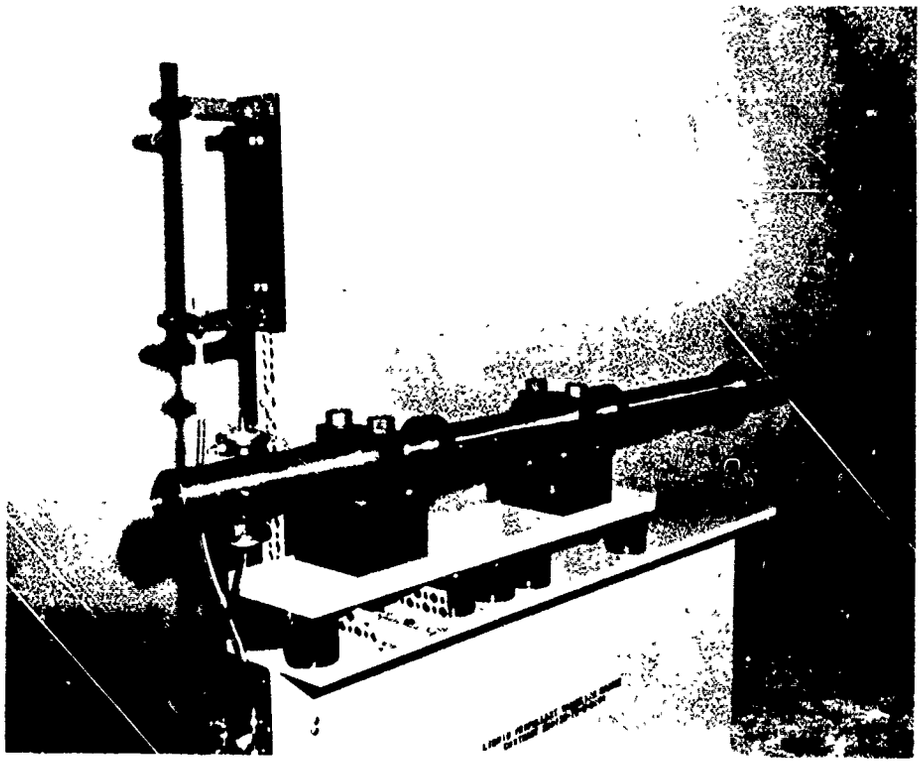

Figure 3.24. Test Fixture

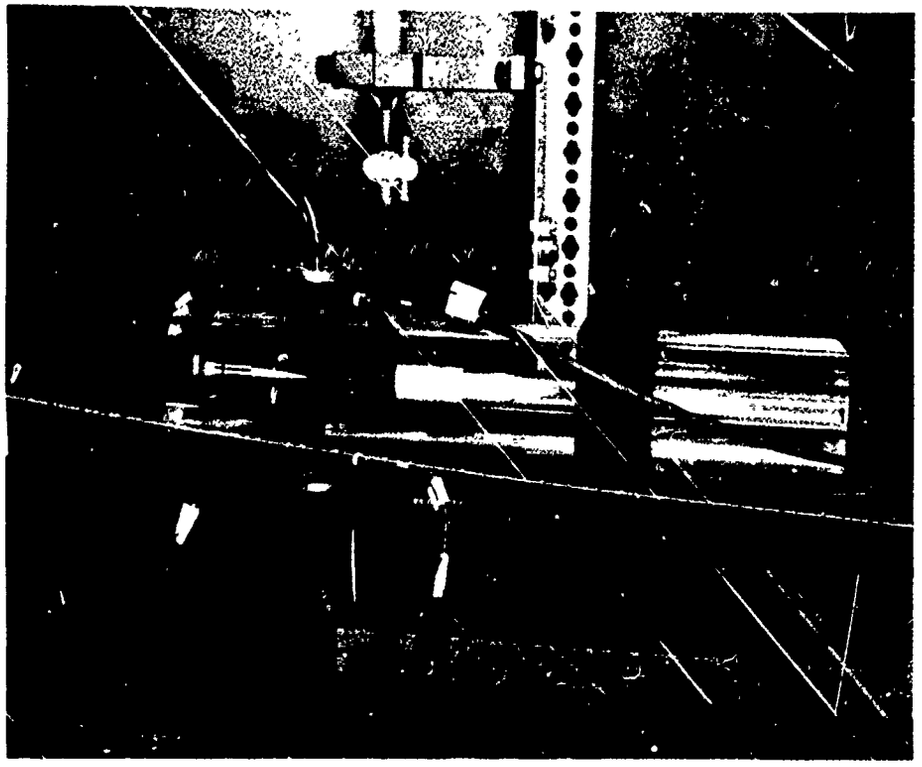

Figure 3.25. Transparent Chamber

When checkout had been completed, the test fixture was moved into the test cell and prepared for firing. Instrumentation was installed. Solenoid valves for controlling the fill, vent and drain valves were mounted on brackets adjacent to the test fixture, rather than on the test fixture itself. This arrangement placed them some distance away in case we wished to hose off the test fixture during the firing program.

Figures 3.26 and 3.27 are photographs showing the test fixture in the test cell ready for firing.

3.2.4 Instrumentation. Parameters measured and the equipment used in their measurement are tabulated in Table 3.5 below.

Table 3.5

Instrumentation

Parameter Measurement	Equipment	Manufacturer	Model Number
Velocity	Ballistic screens	Oehler Research	55
	Computing chronograph	Electronic Counters, Inc.	4001
	Interval timer	Beckman Instruments, Inc.	6001A
	Coils	GE Engineering Development Lab	–
Pressure	Transducers	Kistler Instrument Corp.	607A, 607C2, 207C4, 532, 583C
	Low impedance amplifier system	Kistler Instrument Corp.	
	High impedance amplifier system	Kistler Instrument Corp.	567A, 536, 504H
	Transducer	PCB Piezotronics	118A05
	In-line amplifier	PCB Piezotronics	422M06, 422M07
Projectile Position	Sub-miniature LED Thrubeam pair	SKAN-A-MATIC Corp.	L33007/P33001
Data Records	Oscillograph	CEC	5-133
	Tape recorder	PEMCO	120B
Time Standards	Real time 100 Hz	Assembled by GE Engineering Development Lab using Bulova quartz crystals.	–
	Tape playback 5KH2	Assembled by GE Engineering Development Lab using Bulova quartz crystals.	–

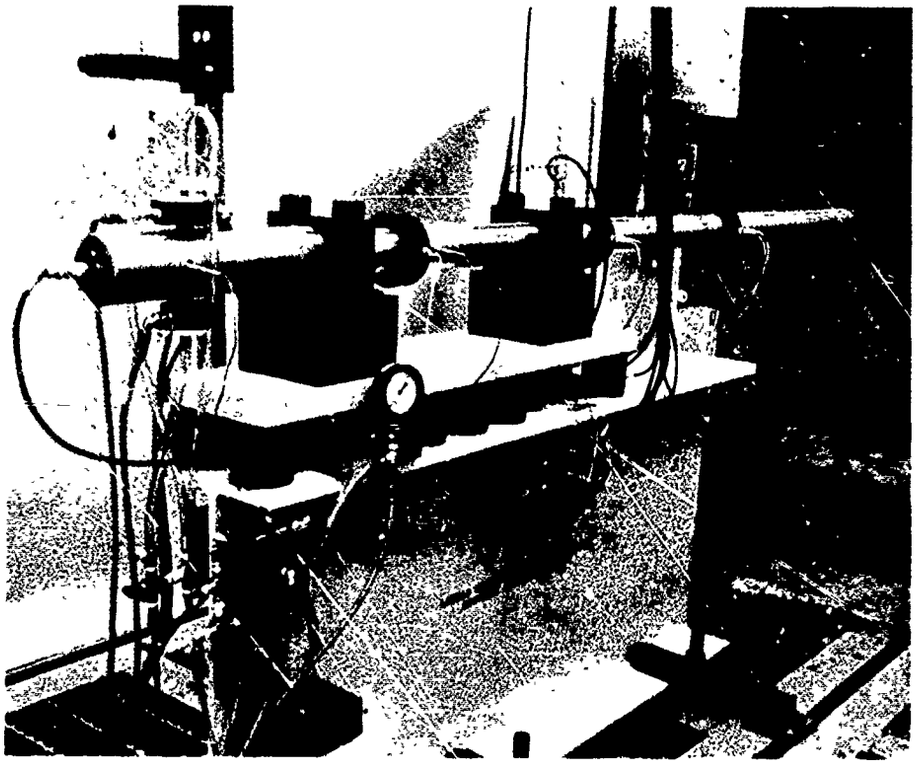

Figure 3.26 Test Fixture in Test Cell

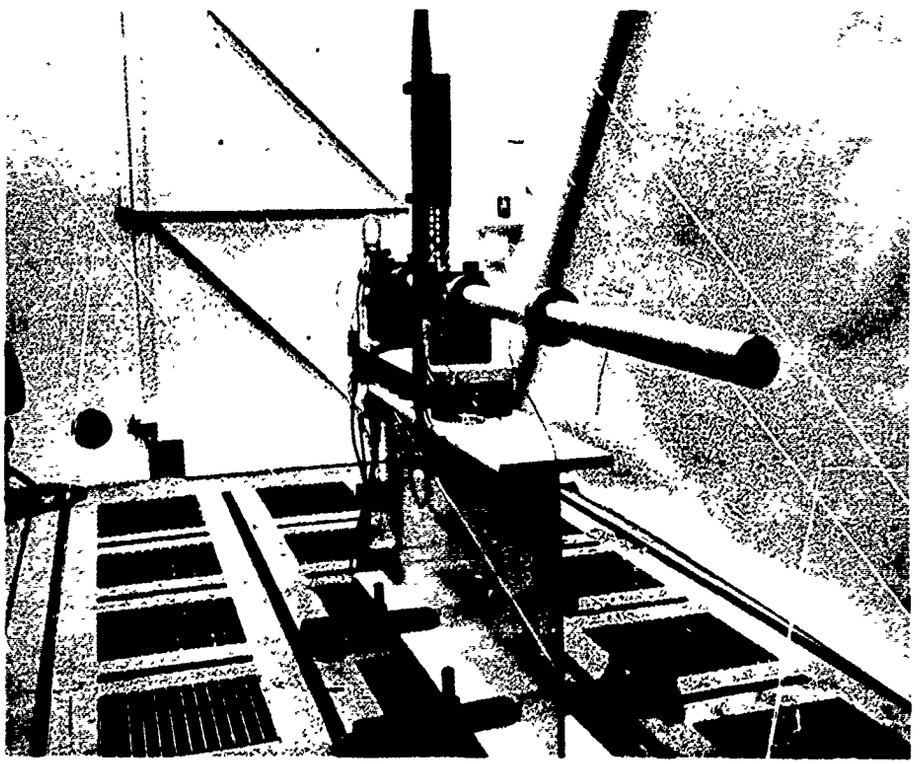

Figure 3.27. Test Fixture in Test Cell

All data were recorded on FM magnetic tape with a Pemco Model 120B recorder. Tape speed was 60 inches per second in recording. Trigger, chamber pressure, light screen signals, muzzle wire, and a 100 Hertz clock pulse were also recorded in real time on a Consolidated Electrodynamics Corporation Datagraph recording oscillograph. Real time data is not particularly useful in analyzing separate events throughout the firing, but it provides a quick check on the validity of the data immediately after a shot.

For data analysis, the FM tape was played back on the recording oscillograph. Tape speed in playback was 3.75 inches per second. Time scaling of the record for convenience in reading was accomplished by adjusting the oscillograph paper speed.

We had originally intended to use only light screens to measure muzzle velocity. However the test cell was a fairly small one, and it had light colored walls. These factors apparently combined to cause occasional premature triggering of one or both light screens from reflected muzzle flash. After we had switched to metallic projectiles, a set of transformer coils was added between the light screens to give an additional indication of projectile passage.

Velocities were calculated in several ways:

1. The light screens triggered the ECI chronograph, which calculated the velocity and gave a digital readout.
2. The light screen signals were recorded on the FM tape. These were played back with an accompanying 500 Hertz timing pulse. The spacing between signals was measured and a velocity was calculated using the 500 Hertz pulse as a time base.
3. Coil signals were recorded on the FM tape and played back. Coil signals spacing was measured on the record and a velocity calculated, again using the 500 Hertz time base.
4. In some firings, a Beckman timer was triggered by the light screens. This permitted a second calculation of velocity directly from the light screen signals, without the need for measuring on a playback record.

Velocity measurements thus had considerable redundancy. Any lack in agreement among the calculations for the same shot was largely the result of visually measuring small intervals on the tape playback record. When the light screen appeared to be working properly, the chronograph velocity was used as the best measurement. The Beckman timer always gave a very close check on this value. When the light screens were not operating correctly, the coils permitted an estimate of velocity.

Fire volts were generally not recorded because associated electrical noise tended to obscure other data momentarily. We did record it once, on Shot 35, to investigate ignition delay. Delay was imperceptible.

3.2.5 Projectiles. Projectile weight was established at a nominal 120gm. This weight is close to representing a 4-pound 75mm launch weight scaled to 30mm in proportion to the cube of the diameter ratio. In addition, considerable data already exists for 120gm 30mm smooth bore firings with NOS365 propellant. We chose a projectile weight which would allow direct comparison between this data and our results.

Teflon projectiles were used in the first firings. Figure 3.28 is a sketch of the design. The projectile had a conical cavity at the rear to generally accommodate the pointed nose of the hollow shell cavity generators. An "O" ring was provided as a seal

Microflash photographs showed that the skirt around the conical recess blew apart as the projectile exited from the muzzle. A change was made to an aluminum projectile with a Lexan sealing skirt. The conical cavity was retained initially. Later, when multiple hole cavity generators were fired, the conical cavity was discarded.

Figure 3.29 shows sketches of the two aluminum projectiles, and Figure 3.30 is a photograph of the type used first.

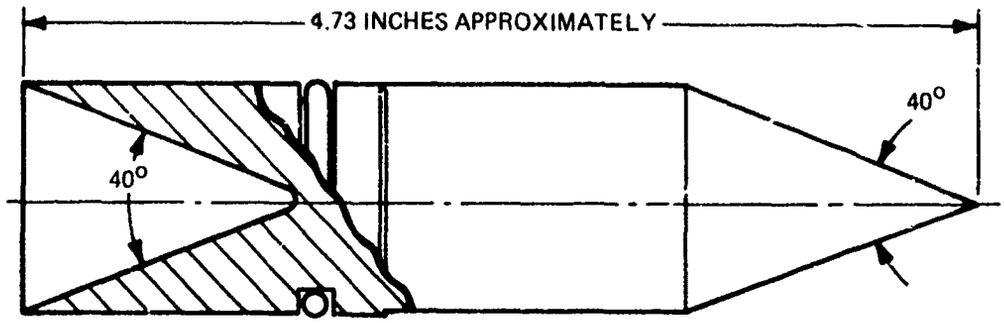

NOMINAL DIAMETER	30MM
WEIGHT	120 GRAMS
MATERIAL	TEFLON

Figure 3.28. Teflon Projectile

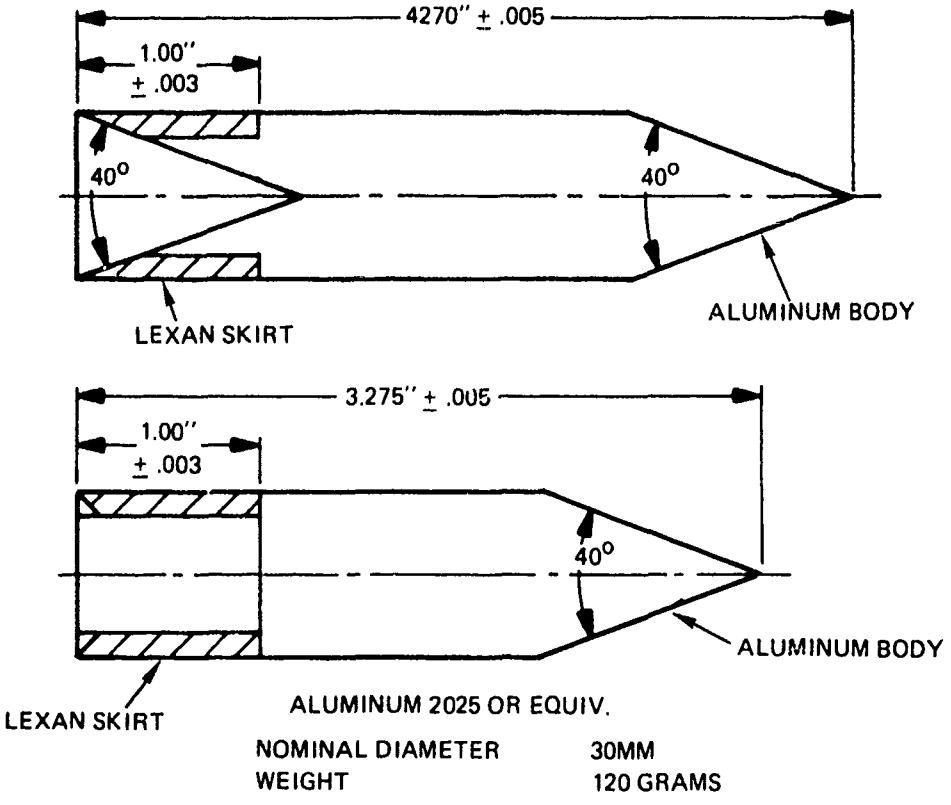

Figure 3.29. Aluminum Projectiles

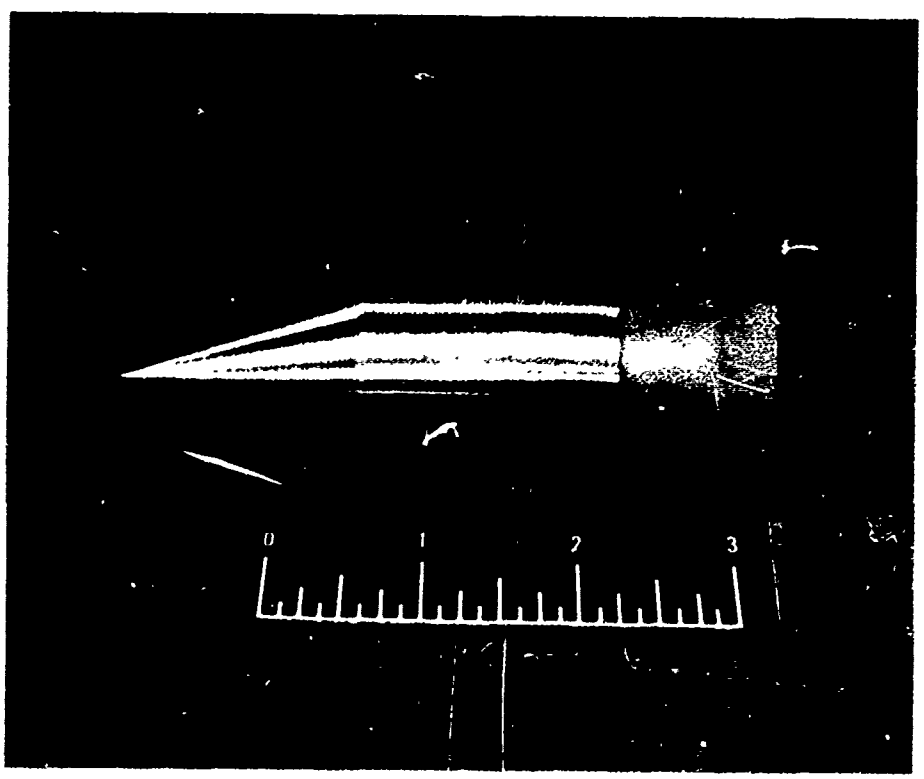

Figure 3.30. Aluminum Projectile

3.2.6 IGNITION BOMB TESTS

3.2.6.1 Solid Propellant Booster. Before firing tests could actually begin in the test fixture, we felt we should determine the quantity of booster charge necessary to generate desired levels of pressure and corresponding temperature in the three cavity generator volumes. For each of the three volumes of interest, varying weights of Hercules Bullseye propellant were ignited in a closed bomb, and chamber pressure was measured. Bullseye propellant was selected because of its rapid burning rate and ready availability. Figure 3.31 summarizes the results.

3.2.6.2 NOS365 Boosters. As discussed in Section 3.2.7.1, the solid propellant booster system did not prove successful. A change was made With solid propellant in the rather large volume of the hollow cavity generators, we were concerned that pressure rise might not be sufficiently rapid. Perhaps the developing combustion was exposed to liquid too soon and was being quenched.

The new approach involved the high-low combustion concept, in which propellant is first burned in a confined space to establish high pressure combustion. Gases from this chamber pass through an orifice to a larger "working" chamber where additional propellant can be burned as a booster or gas expansion work can be done directly at lower pressure.

We decided at the same time to try using NOS365 as the booster charge. Our rationale was that quenching might be less likely if the booster were the same material as the main charge. Whether this feeling is justified is not known, as no comparative studies were made between liquid and solid boosters in the same volume configuration.

The two liquid propellant booster configurations have been described in Sections which deal with breech design. Although we fired the first arrangement without previous testing, we quickly became aware of the need for basic data. We suspended firing briefly to conduct closed bomb tests with the new ignition system. Figure 3.32 is a curve of closed bomb chamber pressure as a function of NOS365 charge weight in the two compartments of the new igniter tube volume.

One calculated point is shown. The curves came so close to the calculated value for this booster configuration that the charge for the second booster arrangement, used with the multiple hole cavity generator, was selected from computation alone.

The liquid propellant booster was so successful in the firing tests that little comparative study was made in evaluating its performance. Whether solid propellant would have served as well in the same situation is not known. Once the change was made to the liquid propellant booster, the firing tests proceeded smoothly with no misfires which could not be accounted for.

3.2.7 Firing Tests. The exploratory nature of the program must be emphasized in introducing this discussion of the firing tests. The cavity generator concept was an untested hypothesis when we began, and at first we did not know what to expect. In a sense, we learned as we proceeded. Adjustments and changes were made when necessary on the basis of observation and sometimes of conjecture. The program became an evolutionary development process, in contrast to a routine following of a pre-established procedure.

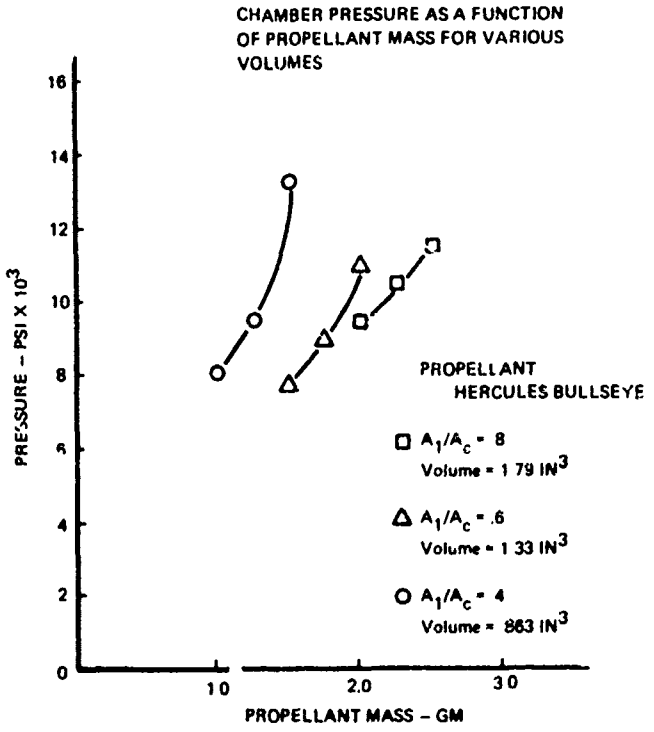

Figure 3.31. Closed Bomb Ignition Booster Test Results for Solid Propellant

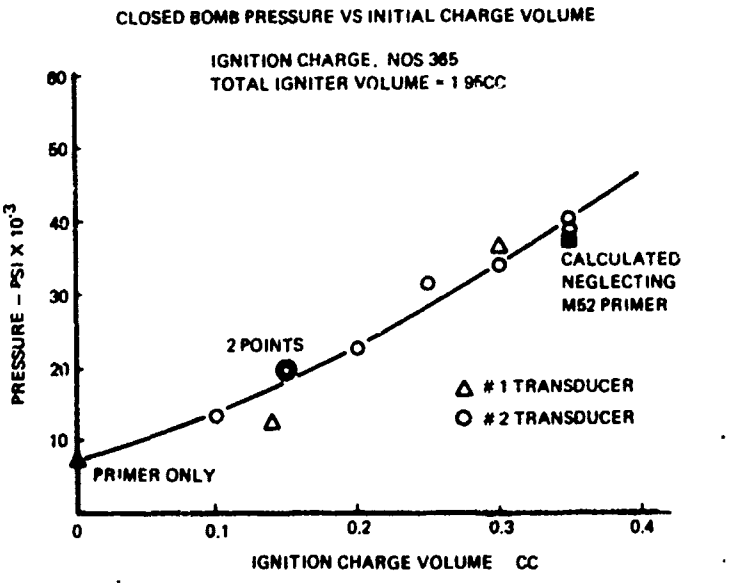

Figure 3.32. Closed Bomb Data for NOS 365 Ignition Charge

Since the program developed in this manner, it seems best to follow the same pattern in outlining it. A chronological narrative will take the reader through developments as they occurred. Reported observations will be seen in true perspective and the stages through which the testing progressed will be made visible in proper sequence.

A total of 40 firings were conducted. They consisted of the following tests:

- 11 with hollow steel cavity generators.
- 22 with multiple hole polypropylene cavity generators.
- 1 with a stationary steel multiple hole orifice plate.
- 1 bulk loaded firing.
- 4 tests without propellant to check booster action.
- 1 misfire.

Appendix 1 is the complete record of all firings.

3.2.7.1 Hollow Shell Cavity Generators. Tests began using the hollow shell cavity generators with Bullseye solid propellant booster charge. For the initial firings in the test fixture, we selected booster charge weights corresponding to 10,000 PSI in the priming volumes. This pressure seemed sufficiently far above the upper transition level from fizz-burn for NOS365 monopropellant.

Four firings were made in the test fixture under these conditions. Two were made with the largest cavity generators, $A_1/A_c = 0.8$; the others used the other two sizes, $A_1/A_c = 0.6$ and 0.4.

Ignition was achieved on all four firings; there were no misfires. However, in all four cases, burning of the main charge was so slow in getting started that the projectile was too far down bore for appreciable pressure to be generated. Pressures were low, muzzle velocities were correspondingly low, and the late burning as the projectile neared the muzzle caused considerable muzzle blast. Projectiles and cavity generators broke apart as they left the muzzle.

Figure 3.33 reflects these effects. It shows pressure time curves for the third and fourth firings. The curves show an initial pressure rise when the booster fires followed by a long delay while combustion barely persists. Finally, when the projectile has progressed quite far down bore – past Station 60 in both cases – pressure increases suddenly. The muzzle is Station 88, for reference. These curves reflected the apparent need to speed up the ignition process in the liquid charge.

The first step taken in trying to speed up ignition of the liquid charge was to increase the booster charge. The next two tests were therefore fired with booster charges corresponding to closed bomb pressures of 15,000 psi and 20,000 psi respectively. Although the resulting primer pressure peaks were higher than on previous firings, delayed burning was still observed. Shots 7 and 8 in Figure 3.34 show the two pressure time curves.

It will be noted that even when the firing pressure was 14,000 psi, which is far above the reported limits of the Fizz-burn mode, delayed burning was encountered.

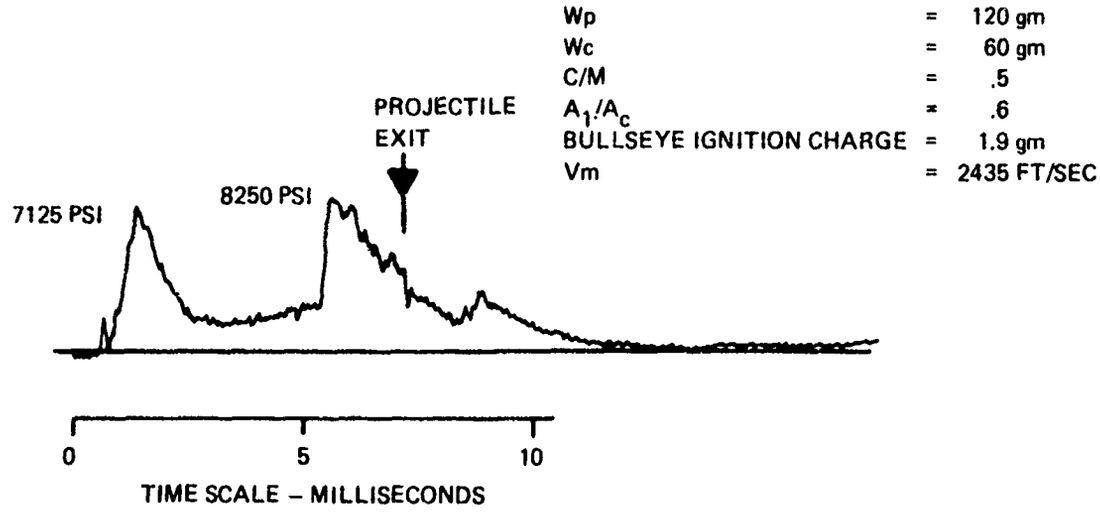

PRESSURE-TIME CURVE FOR SHOT NUMBER 5

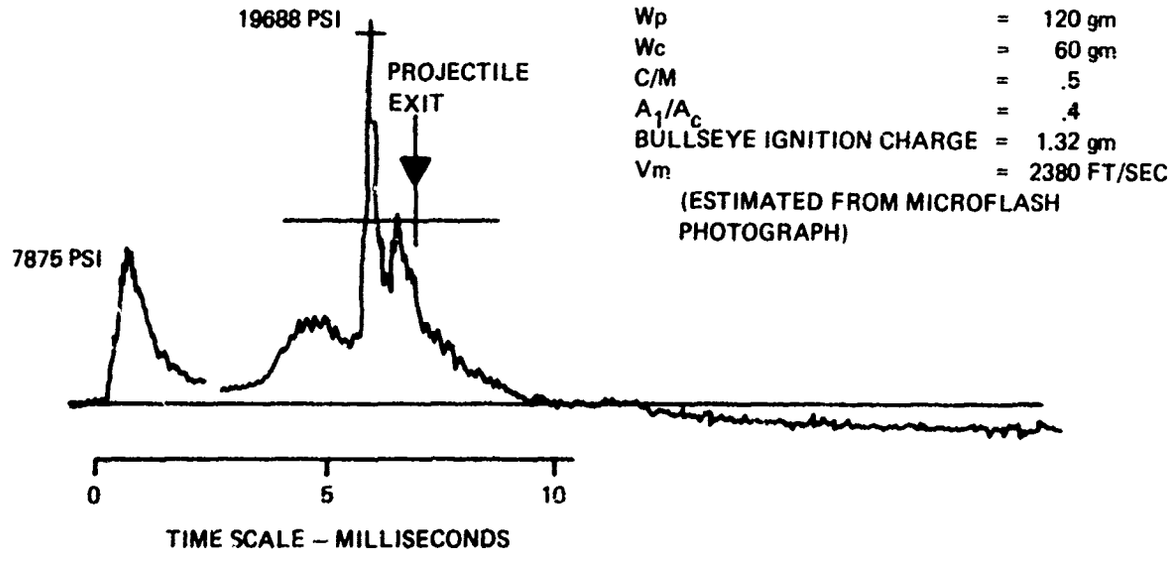

PRESSURE-TIME CURVE FOR SHOT NUMBER 6

Figure 3.33. Typical Firing Data for Hollow Shell Cavity Generators -- Solid Propellant Booster Charge Corresponding to 10,000 psi

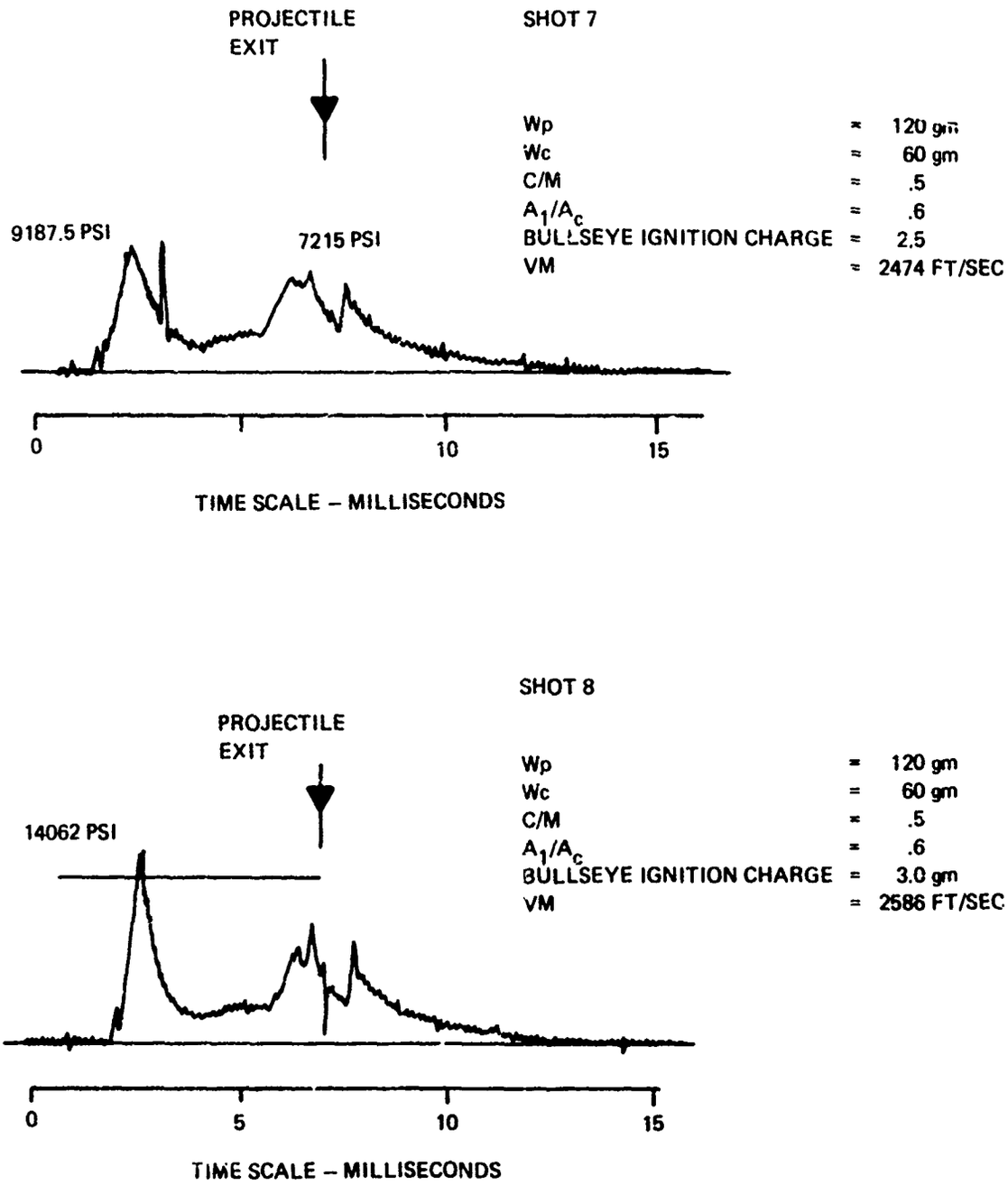

Figure 3.34. Typical Firing Data for Hollow Shell Cavity Generators – Increased Solid Propellant Booster Charges

With solid propellant booster charges not successful, a change in priming system was made. We reasoned that burning might be initiated more successfully if some portion of the main charge was located behind the cavity generator before firing. The main body of the charge would then be ignited earlier. We changed the breech design to the second type described earlier, in which the cavity generator is actually immersed in the main charge and the booster charge ignites a portion of the liquid within the cavity generator. This design was described in Section 3.2.1.

In the first firing conducted with this system, Shot 9, we used a total charge of 0.5cc of NOS365, 0.14cc in the small volume, and the balance in the large volume. A middle-sized cavity generator was used.

The shot turned out to be a bulk-loaded firing. The booster charge, together with that portion of the main liquid charge trapped behind the nose of the cavity generator, apparently blew out the nose of the cavity generator. Ignition of the bulk of the main charge immediately followed. Muzzle velocity and chamber pressure data are not considered reliable for that particular shot, but estimates are 3500-4000 ft/sec. and over 45,000 psi respectively. Action time from ignition to muzzle exit was markedly reduced from the early series of firings, indicating a high-pressure, rapid buildup and higher muzzle velocity.

Feeling that our booster charge was now much too energetic, we suspended firing briefly to conduct the closed bomb tests which have been described in Section 3.2.6.2. The tests showed that the 0.5cc ignition charge first used corresponded to a quite high pressure.

A second shot, T10, was fired using a 0.25cc ignition charge. A change in cavity generator size was also made between the two firings, because the last middle-sized cavity generator had been used in 9. Experience was much the same as on the previous firing. The pressure time curve is shown in Figure 3.35. It has all the characteristics of a bulk-loaded firing.

Three changes were now considered as possible measures to reduce the initial ignition energy and soften the ignition process. One was to reduce the quantity of propellant within the nose of the cavity generator immediately ahead of the igniter tube. A second was to simply reduce the size of the ignition charge in the igniter tube. A third was to angle the exit holes from the igniter tube rearward rather than having the ignition gases aimed directly at the nose of the cavity generator.

To evaluate the first change, the quantity of propellant in the nose of the cavity generator was reduced by placing some styrofoam ahead of the igniter tube in the nose of the cavity generator. This displaced fluid and reduced the amount of liquid charge in that region. The result was a Fizz-burn followed by an extremely rapid rise to 62,500 psi chamber pressure. The pressure-time curve is shown in Figure 3.36, labeled as Shot 11. Apparently, the reduction of charge in the nose of the cavity generator reduced the energy of the initial ignition, and we repeated the experience of the earlier Bullseye shots, except at a very much higher energy level and within a much shorter time interval.

The second firing evaluated the affect of simply lowering the ignition charge inside the igniter tube. Igniter charge was reduced to 0.1cc. This had the same affect as the styrofoam filler in the cavity generator. Fizz-burn persisted for about 2 milliseconds. Then a rapid rise occurred, this time to 111,250 psi. A high-speed movie of the muzzle on this shot shows considerable blast.

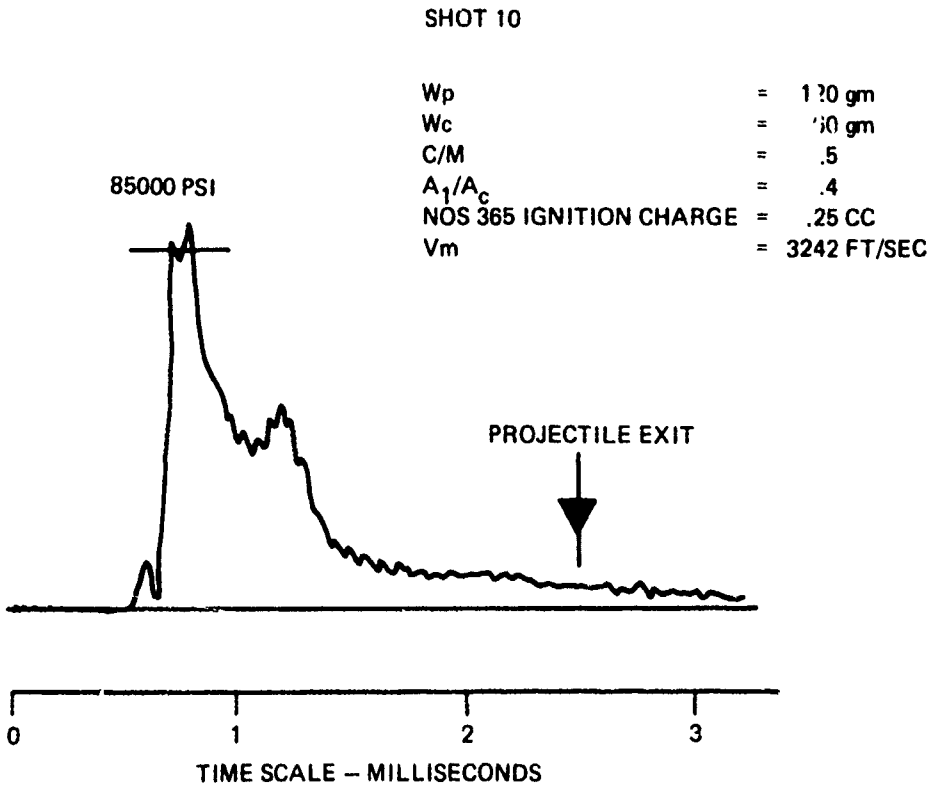

Figure 3.35. Firing Data for NOS 365 Ignition System

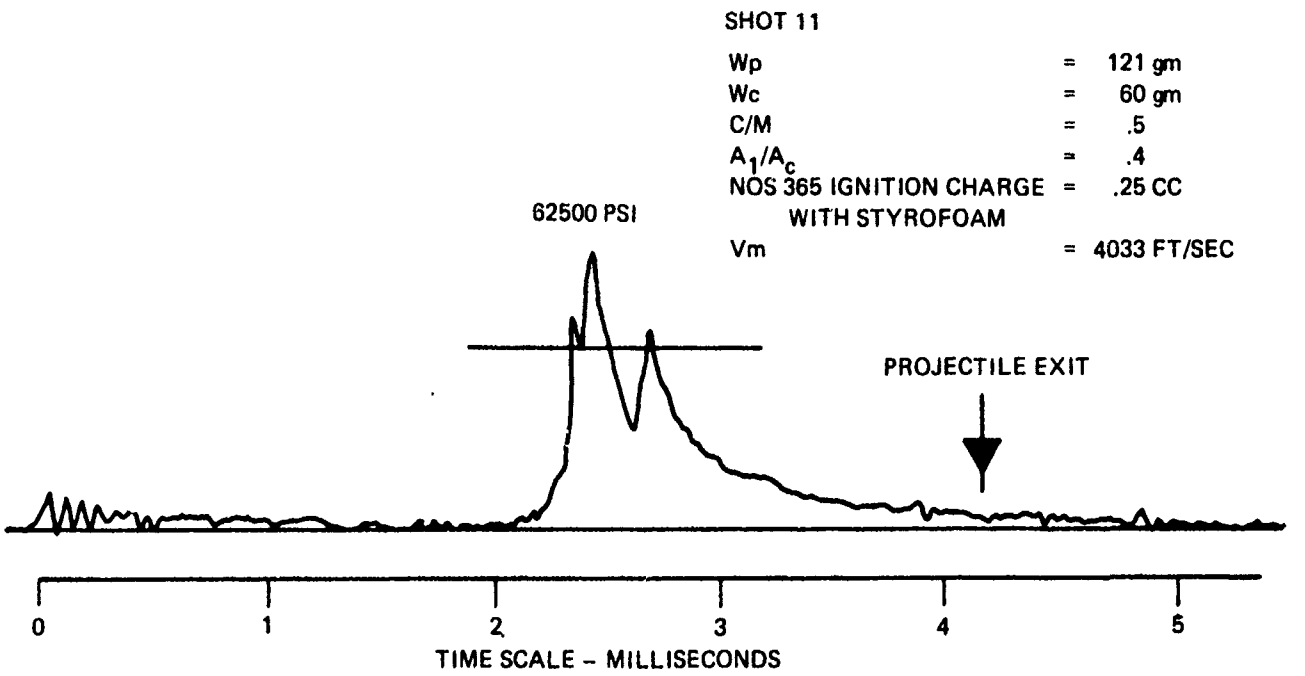

Figure 3.36. Firing Data for Styrofoam Filler

The flash apparently triggered the second ballistic screen prematurely, for the chronometer indicated 4813 ft/sec. muzzle velocity. Estimates of muzzle velocity from other events indicate that it was probably nearer 4000 ft/sec. The pressure time curve for this firing is shown in Figure 3.37.

The third method mentioned as a means of adjusting ignition, angling the ignition holes rearward, required a new igniter tube. A new tube was fabricated. Where the central tube had originally opened forward, presumably igniting propellant inside the tip of the cavity generator, angled holes now directed the ignition flame rearward. The intent was to start combustion within the main body of propellant inside the cavity generator rather than in the somewhat confined nose region. A drawing of this tube was shown in Figure 3.17.

A shot fired with this arrangement was not successful. Low pressure, delayed burning was again encountered. A large cavity generator was used, as no intermediate or small ones were left. Figure 3.38 shows the pressure-time curve and pertinent data for the firing. Since this was our next to last steel cavity generator, testing of shell-type stainless steel cavity generators was terminated.

From the trend of the discussion, it should be clear that testing so far had revealed the traveling charge effect to not be operating in the manner intended. There was unmistakable evidence that the presence of the cavity generator does affect the dynamic behavior of the charge, and that the sharp initial rise of pressure associated with bulk-loaded firings can be delayed. Some control over the ignition process should therefore be possible. However, none of the ignition schemes yet tested had been able to control burning in the desired manner.

Observations seemed to indicate that the shell-type cavity generator leaves too little fluid surface exposed early in the firing process. This surface would be expected to be in the form of a simple cylindrical sheath of propellant along the wall behind the cavity generator. We decided that another surface configuration might be worth investigating.

3.2.7.2 Multiple Hole Cavity Generator Tests. The basis for deciding to use multiple-hole cavity generators and the details of the designs developed for testing have been discussed in Section 3.1. The various configurations evolved gradually. Tests began tentatively with a single trial. When results reflected promise, new designs were tried and changes were made to improve procedures. The objective was to learn as much as possible, in a limited number of firings, about the influences of shape, size and proportion upon ballistic performance.

In most cases, more than one shot was fired at a given set of conditions. Although the statistical sample could not be large, a rough idea of repeatability could be gained. Table 3.6 repeats the list of configurations from an earlier section and indicates the number of shots fired with each. The table indicates that one firing was made with a stationary steel cavity generator or orifice plate and that one bulk-loaded shot was fired. These last two were made to allow comparison between firings with and without cavity generators.

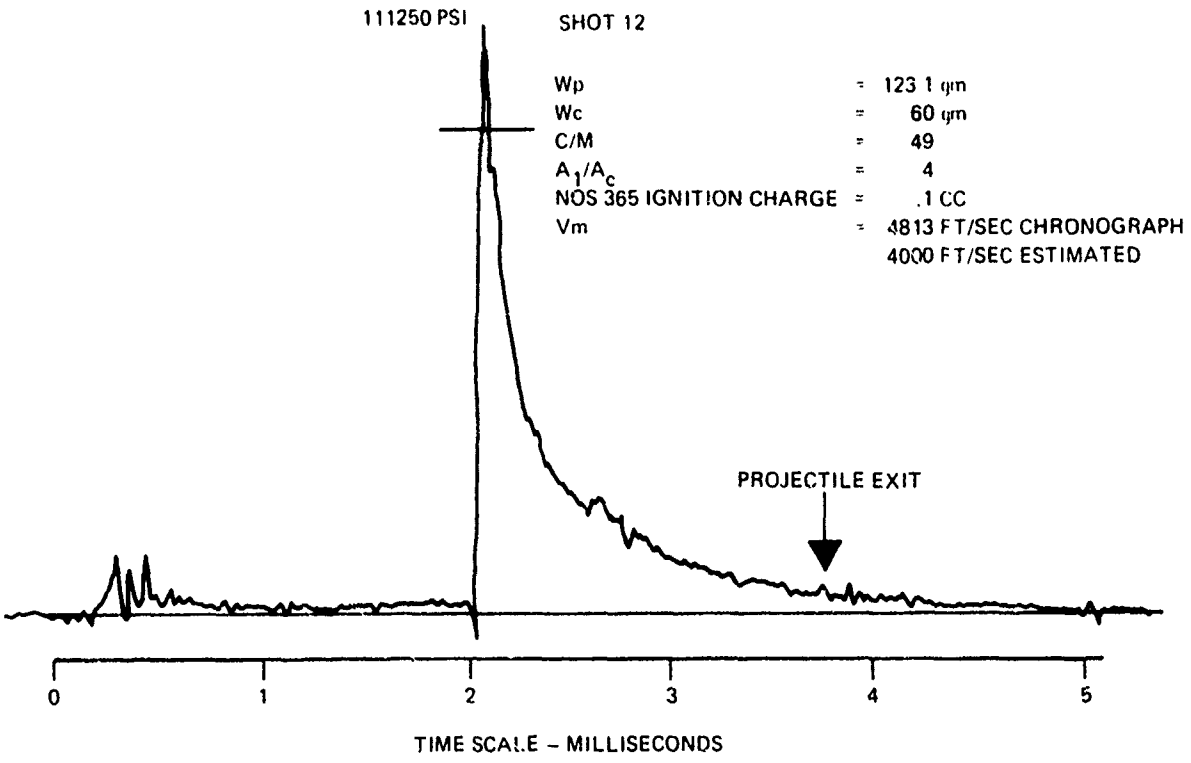

Figure 3.37. Firing Data for Reduced Ignition Charge

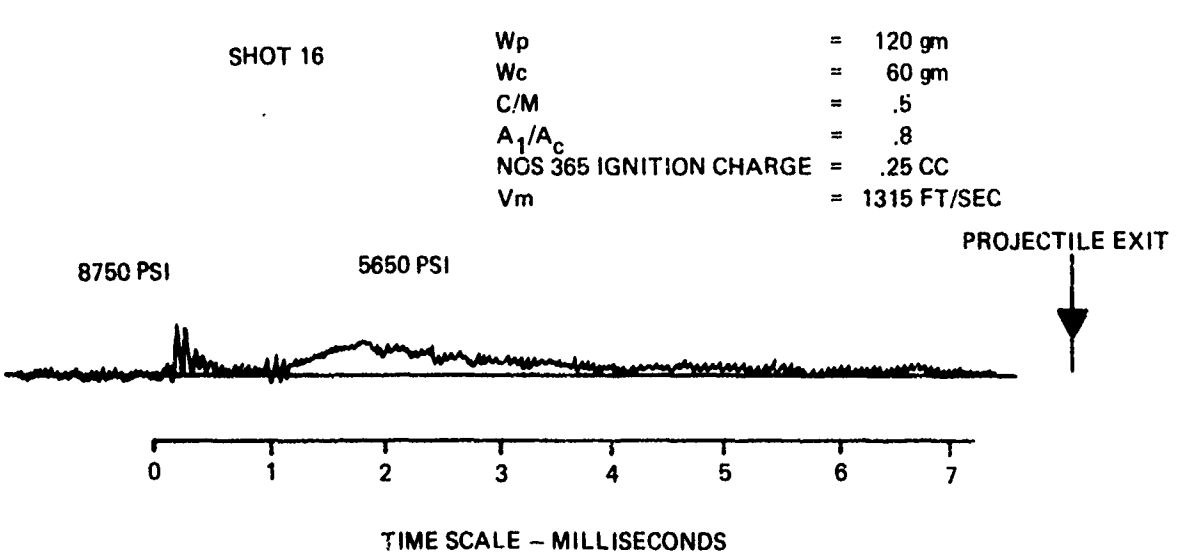

Figure 3.38. Firing Data for Rearward Directed Ignition Holes

Table 3.6

Multiple Hole Cavity Generators Fired

Configuration	Shots Fired
19-hole circular. No skirt. 1-inch long. Fired at C/M = .5.	1
19-hole circular. Attached skirt. 1-inch long. C/M = .75, and 1.0.	6
19-hole circular. Separate skirt. 1-inch long. C/M = .75.	3
36-hole circular. Separate skirt. 1-inch long. C/M = .75.	3
19-hole circular. Separate skirt. 2-inches long. C/M = .75.	3
19-hole hexagonal. Straight holes. Separate skirt. C/M = .75. 1-inch long.	3
19-hole hexagonal. Tapered holes. Separate skirt. C/M = .75. 1.375 inch long.	3
Stationary steel. 18-hole. 1-inch long.	1
Bulk loaded. No cavity generator	1

Description of the tests will follow the order of the table, although the firings were not necessarily conducted in that order. Appendix I lists the actual order of firing.

19-Hole Circular. No Skirt. 1 Inch Long. C/M = 0.5

The first firing was at a C/M of 0.5. A double hump pressure time curve was obtained, with a peak pressure of 59,375 psi. Muzzle velocity was measured by the chronograph as 4305 feet per second. The double hump characteristic of the pressure time curve still resembled the delayed ignition characteristic of the earlier firings, but on a much shortened time scale. Data for the firing are shown in Figure 3.39.

Debris from the cavity generator left the muzzle and was found on the floor of the test cell after the firing. The plug had separated into slivers formed from the interstices between holes. The slivers were still one inch long, indicating that the polypropylene had not compressed appreciably in a lengthwise direction.

The drop in pressure after the initial peak suggested, in a superficial way, that the cavity generator might still be "outrunning" the combustion process. We reasoned that increasing the charge might reduce this apparent tendency by slowing the acceleration with a heavier mass.

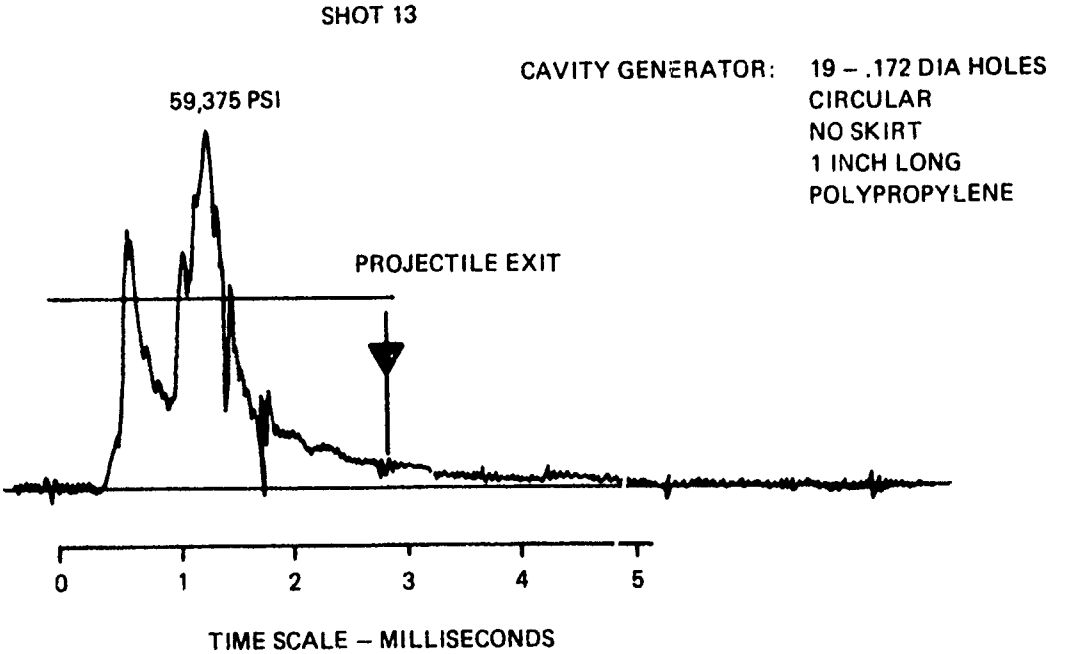

SHOT	Wp gm	Wc gm	C/M NOMINAL	A/A_c	Pc LB/IN^2	Vm FT/SEC
13	115	60	.5	.6	59375	4305

Figure 3.39. Firing Data for 19-Hole Cavity Generator C/M = .5

19-Hole Circular. Attached Skirt. 1 Inch Long. C/M = 1.0, and 0.75

A skirt was added to the cavity generator to permit it to be secured to the primer support.

The next series of three firings were conducted at C/M = 1.0. Pressures and velocities were higher.

Unfortunately, after the first shot at C/M = 1.0, we began having trouble with pressure transducers and the tape recorder. We did not successfully record chamber pressure on the next two shots. The third firing had a slightly lower velocity, but little generalization is possible on the basis of the data taken.

Surprisingly, the cavity generators remained in the bore after all three shots. They were still more or less intact, as well. Their position varied, but they were somewhere forward of the breech face on at least the last two shots. On the first shot, we pushed the plug out with a ramrod before realizing it was there.

The velocities measured on these shots are significantly higher than had been expected at these values of C/M after comparison with other data. In addition, we do not fully understand why the cavity generators remained in the bore after the three shots at C/M = 1.0. Apparently, combustion occurs ahead of the cavity generator as well as behind it, but the time history of events is still not clear.

The charge-to-mass ratio was reduced to 0.75 for the next three shots. Muzzle blast at C/M = 1.0 was a problem in the fairly confined test cell in which the firing was conducted. We felt that although lowering the charge-to-mass ratio would result in somewhat lower performance, data would still allow observation of the trends and provide valid information.

Unfortunately, transducer problems were still encountered. Even with the addition of a second transducer in the chamber, we were not successful in measuring chamber pressures on the next three firings. Adjustment in transducer seats and connector installation finally resolved this problem and satisfactory chamber pressures on at least one transducer were more reliable thereafter until near the end of the progra n.

Experience with down-bore pressure transducers was less successful. These transducers are another type, which had to be used because a shallower installation was necessary in the thiner wall down-bore. Although the transducers calibrated well, they were more susceptible to damage from lateral accelerations during firing than those used in the chamber. After they had been used for a time, we observed that tapping them on the side created considerable noise. This was probably less a problem with the piezoelectric crystal itself than with the attachment from the crystal to the connector. Whatever the cause of the problem, the original supply of down-bore transducers was exhausted, and our down- bore pressure records are not complete.

In the firings at C/M = 0.75, the cavity generators no longer remained in the bore after firing. They were expelled from the muzzle and would be found on the test cell floor after firing. They no longer splintered as they had at C/M = 0.5. They were more or less intact, apparently suffering little more than impact damage.

Firing data for this series of firings is shown in Figure 3.40. As mentioned above, pressure-time traces were not successfully recorded in five of the shots.

19-Hole Circular. Separate Skirt. 1 Inch Long. C/M = 0.75

A second variation was then adopted in order to facilitate the loading procedure. The skirt was separated from the cavity generator and made a separate piece. This approach allowed the use of a flexible polyethylene membrane secured under the skirt to provide a seal at the rear of the cavity generator. Since this constituted a minor design change, a series of three shots was repeated with this configuration. Primary design was still 19-holes in a 1-inch long cavity generator. Figure 3.41 shows the firing data for this series of shots. A fair degree of similarity is noted among the pressure time traces, and muzzle velocities are within 136 ft/sec of one another. No effect from separating the skirt from the cavity generator is apparent.

36-Hole Circular. Separate Skirt. 1 Inch Long. C/M = 0.75

Next, a series of three firings was conducted to investigate the effect of changing hole size. A cavity generator design with 36 smaller holes was substituted for the 19-hole design. Hole diameter was adjusted so that total hole areas were identical for both 19-hole and 36-hole cavity generators. Thus, the ratio of cavity generator area to bore area, A_1/A_c was preserved at a value of .6.

Figure 3.42 shows the firing data for these firings. Chamber pressure traces are similar to those for the 19 larger holes. Two velocities are lower and one higher than for the 19-hole design, however. Both coils and screens worked on all three shots, so no reason is apparent for the higher velocity spread.

CAVITY GENERATOR: 19 – .172 DIA HOLES
CIRCULAR
ATTACHED SKIRT
1 INCH LONG
POLYPROPYLENE

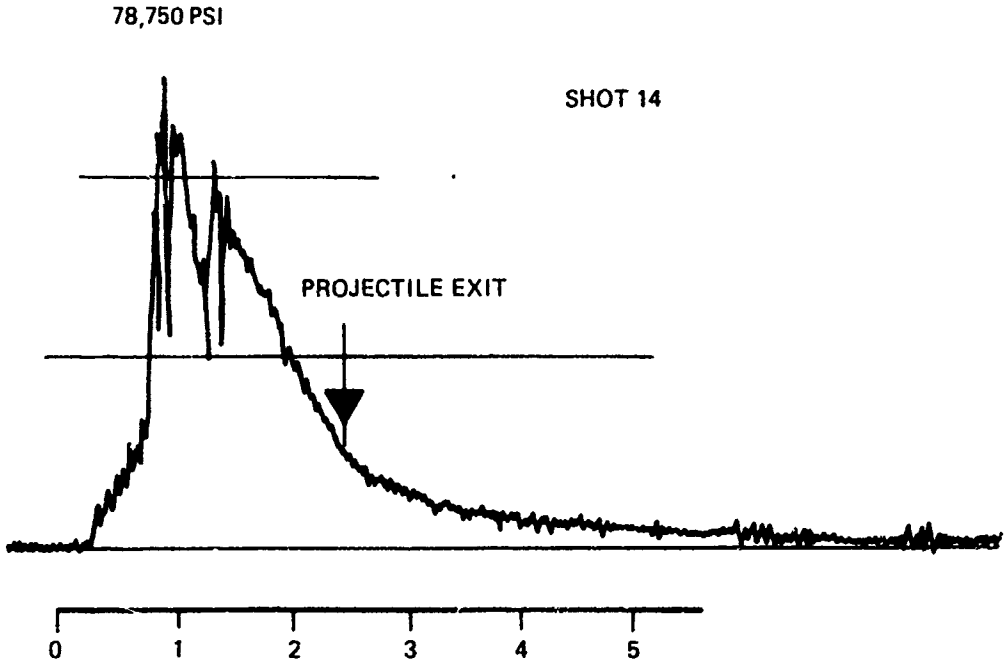

SHOT	Wp gm	Wc gm	C/M NOMINAL	A/A_c	Pc LB/IN^2	Vm FT/SEC
14	115	120	1.0	.6	78750	5710
17	123.2	120	1.0	.6		5765
18	123.2	120	1.0	.6		5545
21	125	90	.75	.6		5300*
22	125.2	90	.75	.6		4942
23	124.8	90	.75	.6		4549

* PROBABLY NOT ACCURATE – SEE APPENDIX 1

Figure 3.40. Firing Data for 19-Hole Cavity Generator C/M = 1.0 and .75

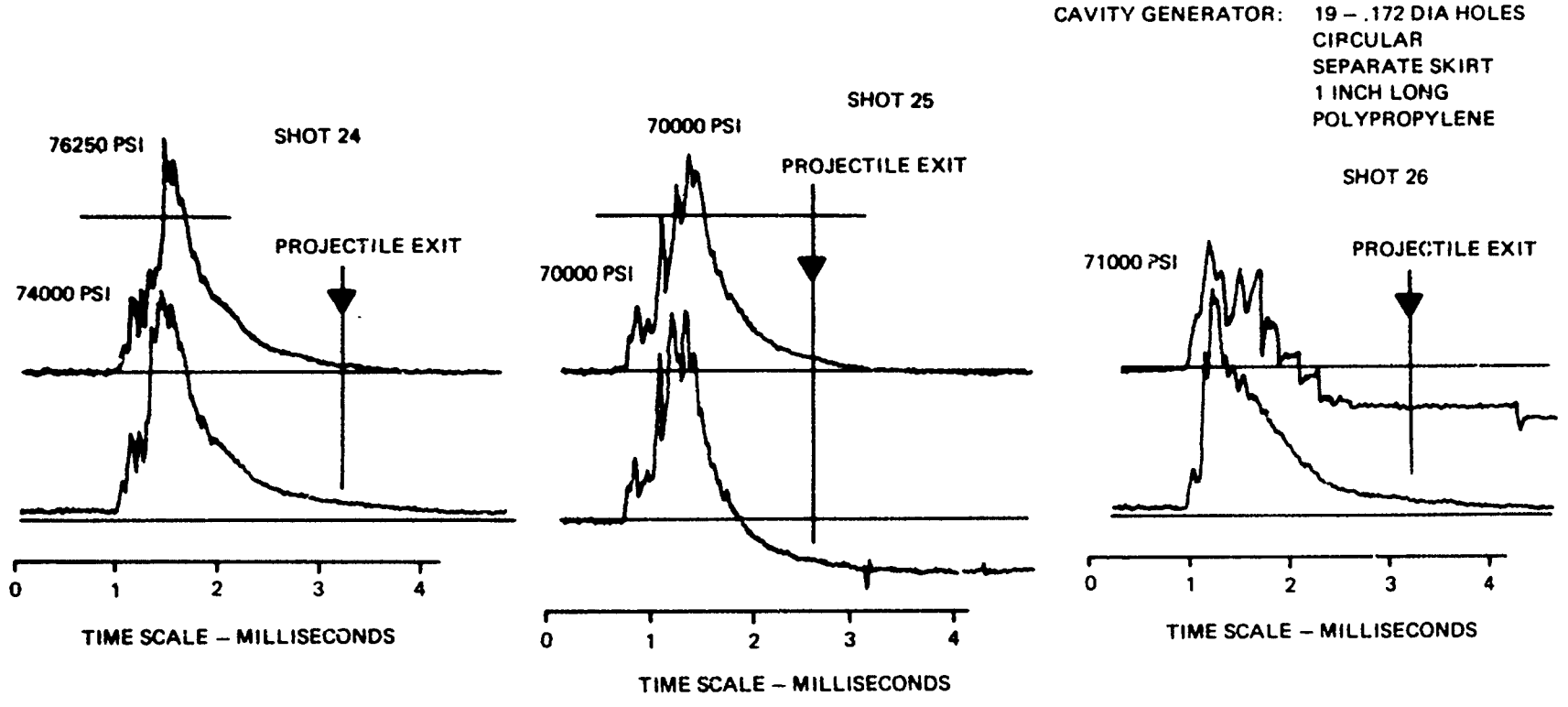

SHOT	Wp gm	Wc gm	C/M NOMINAL	A/A_c	Pc LB/IN^2	Vm FT/SEC
24	125	90	.75	.6	76250	4656
25	125	90	.75	.6	70000	4726
26	124.3	90	.75	.6	71000	4591

Figure 3.41. Firing Data for 19-Hole Cavity Generator -- Separate Skirt C/M = .75

CAVITY GENERATOR: 36 – .125 DIA HOLES
CIRCULAR
SEPARATE SKIRT
1 INCH LONG
POLYPROPYLENE

SHOT 27

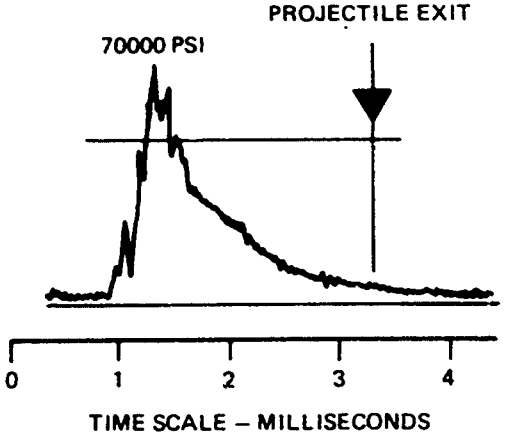

SHOT 28

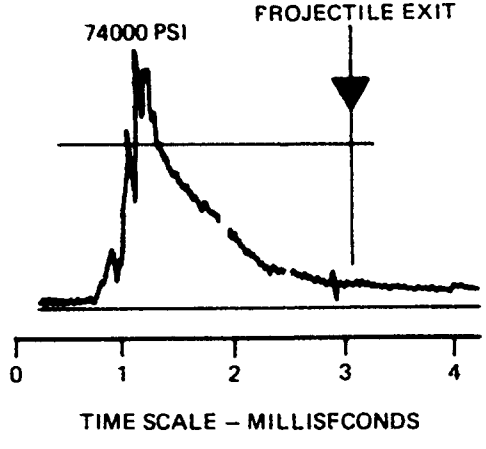

SHOT 29

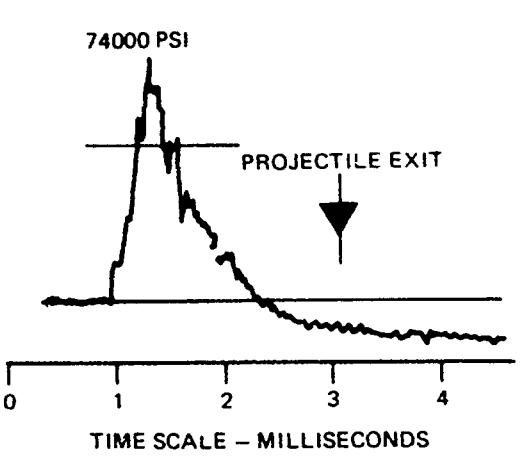

SHOT	Wp gm	Wc gm	C/M NOMINAL	A/A_c	Pc LB/IN^2	Vm FT/SEC
27	125.4	90	.75	.6	70000	4407
28	125.4	90	.75	.6	74000	4404
29	125.6	90	.75	.6	74000	4813

Figure 3.42. Firing Data for 36-Hole Cavity Generator C/M = .75

19-Hole Circular. Separate Skirt. 2 Inches Long. C/M = 0.75

Three shots used a 2-inch long cavity generator which duplicated the latest 19-hole design in other respects. The objective was to observe the effect of cavity generator length on ballistic performance.

Two shots had low velocities, and only one satisfactory pressure-time trace was obtained. Figure 3.43 summarizes the firing data.

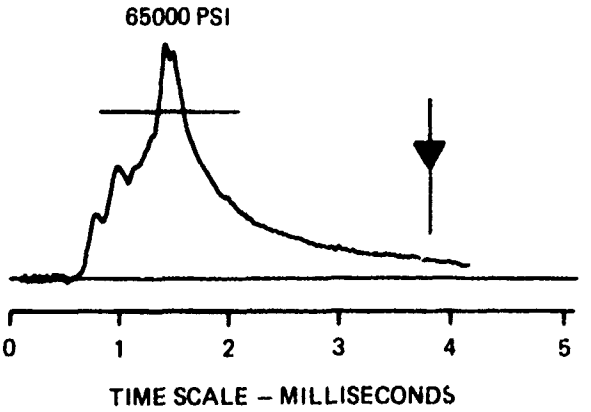

SHOT 31

CAVITY GENERATOR: 19 – .172 DIA HOLES
CIRCULAR
SEPARATE SKIRT
2 INCHES LONG
POLYPROPYLENE

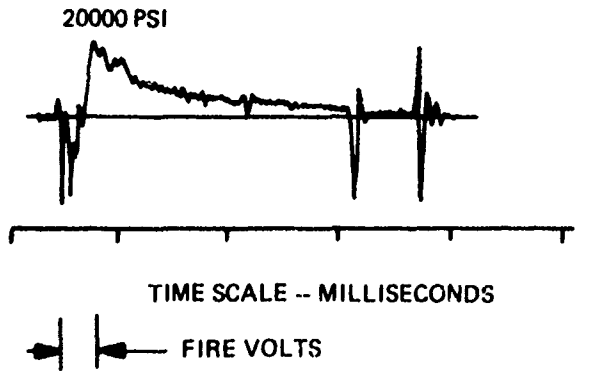

SHOT 35

PEAK PRESSURE MAY HAVE BEEN OBSCURED BY NOISE FROM FIRE VOLTS. HIGHEST READING WAS 20,000 PSI ALTHOUGH PRESSURE MAY HAVE BEEN FALLING AT THAT TIME.

SHOT	Wp gm	Wc gm	C/M NOMINAL	A/A_c	Pc LB/IN^2	Vm FT/SEC
31	124.2	90	.75	.6	65000	3047
34	125	90	.75	.6	(ERRATIC TRACE)	4400
35	125	90	.75	.6	20000 (SEE COMMENT)	1385

Figure 3.43. Firing Data for 2-Inch Long Cavity Generator C/M = .75

The higher pressure time curve exhibits a considerably slower rate of rise than those for the shorter cavity generators, although peak pressure is about the same. A conclusion might be drawn that the longer hole passage through the cavity generator slows the action during firing. However, the poor agreement between this and the other firings makes any interpretation questionable. More data will be required before the effect of cavity generator length can be assessed.

19-Hole Hexagonal. Straight Holes. Separate Skirt. 1 Inch Long. C/M = 0.75

Three shots were fired with a hexagonal design. The objectives was to investigate the effect of leaving propellant along the bore surface during cavity generator motion. The circular cavity generator design was modified by machining sectors off the round cylinder to make the exterior of the cavity generator a hexagon. Thus, the cavity generator contacted the wall at only six points. This contact was retained to provide guidance.

Figure 3.44 shows the firing data for this series. The pressure time curve for the first firing was the most successful pressure-time curve of the complete multiple hole series. The rate of rise of pressure is relatively gentle, peak value is reasonable, and there are no spikes or double humps exhibited in the burning. Unfortunately, the next two shots did not confirm the first. The pressure-time record for the second is not considered reliable, and the third shot is another low pressure, low velocity shot. Apparently, most of the propellant did not burn but was blown out the muzzle. A plate between muzzle and the velocity screens was wetted by unburned propellant.

19-Hole Hexagonal. Tapered Holes. Separate Skirt. 1.375 Inches Long. C/M = 0.75

This cavity generator design used tapered holes in an attempt to investigate the effect of passage shape. Holes tapered from 0.125 inch diameter at the base to a diameter at the front equal to the pitch between holes. The front of the cavity generator therefore presented sharp edged openings for the fluid to enter. Length was increased to maintain the same total displacement volume. Thus area ratio and displacement volume were identical to those of the previous groups. Only the hole shape was different. The firings are summarized in Figure 3.45.

None of this group of firings gave satisfactory results. Because of the shape, the hexagonal cavity generators are much more difficult to load and install. Possibly we introduce some variability at this point. Leakage may have occurred through or behind the separating membrane without our knowledge, between the time we installed the primer support and the firing. A new primer support design could eliminate much of the manual manipulation presently required in loading this design.

Steel Orifice Plate

One firing was conducted with a steel "cavity generator" attached to the breech face by means of a threaded stud. The cavity generator was intended to remain stationary and to act as an orifice plate. The purpose of the firing was to check the effect of motion of the cavity generator in a typical firing. Since the cavity generators had not left the bore at larger charge-to-mass ratios, a question arose as to whether cavity generator motion is significant during the firing process. We felt that using a heavy cavity generator much denser than the propellant and attaching it securely to the breech face might reveal something about the effect of motion, if any, during the firing process.

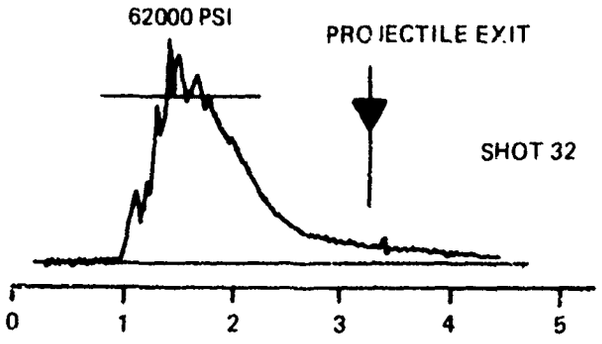

CAVITY GENERATOR: 19 – .125 DIA HOLES
HEXAGONAL
SEPARATE SKIRT
1 INCH LONG
POLYPROPYLENE

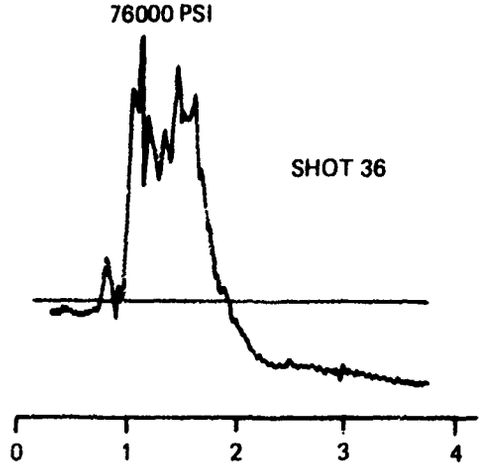

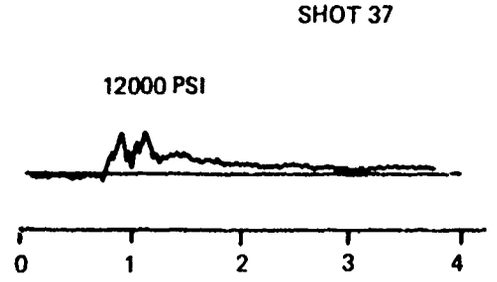

SHOT	Wp gm	Wc gm	C/M NOMINAL	A/A_c	Pc LB/IN^2	Vm FT/SEC
32	123.8	90	.75	.6	62000	4637
36	125	90	.75	.6	76000	4771
37	125	90	.75	.6	12000	1472

Figure 3.44. Firing Data for Hexagonal Cavity Generator with Straight Holes C/M = .75

CAVITY GENERATOR: 19 – .125 DIA HOLES AT BASE
HEXAGONAL
SEPARATE PART
1.375 IN [illegible] LONG
POLYPROPYLENE

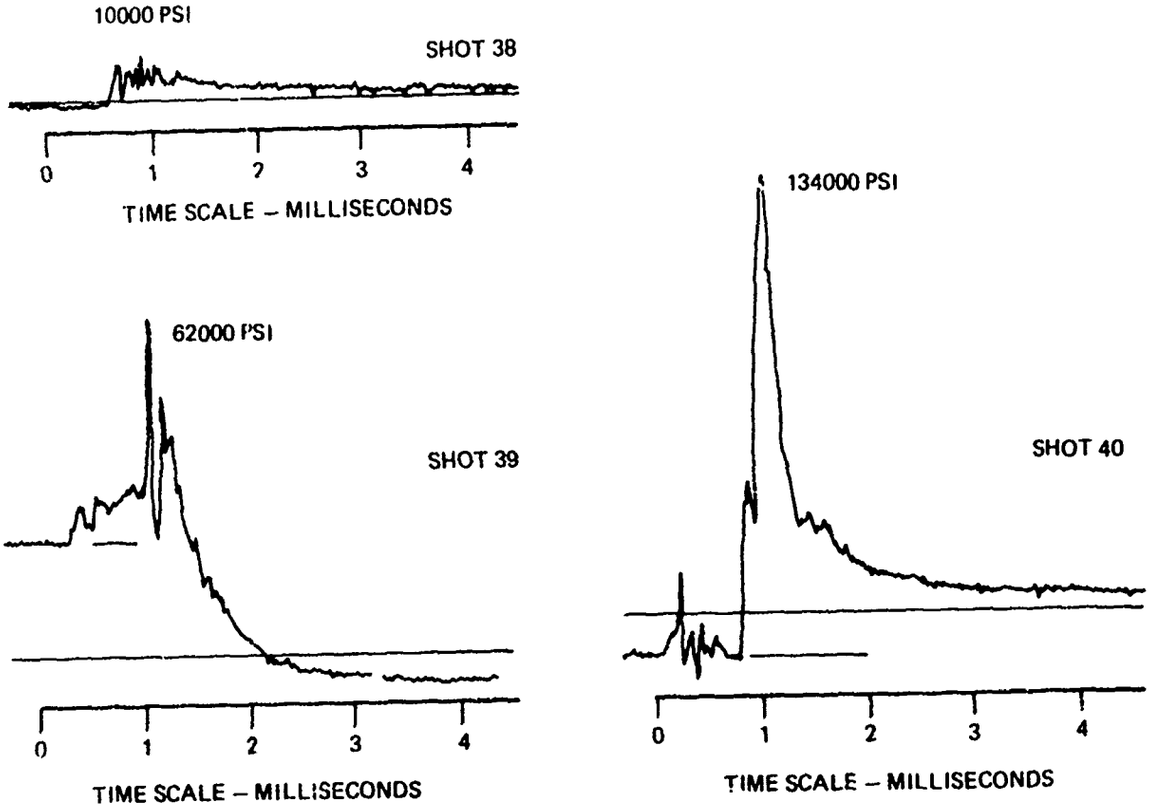

SHOT	Wp gm	Wc gm	C/M NOMINAL	A/A_c	Pc LB/IN^2	Vm FT/SEC
38	125	90	.75	.6	10000	1535
39	125	90	.75	.6	62000	2105
40	125	90	.75	.6	134000	4266

Figure 3.45. Firing Data for Hexagonal Cavity Generator with Tapered Holes C/M = .75

Figure 3.46 is a photograph of the steel cavity generator orifice plate, the primer support, and the attaching stud. The cavity generator was machined to the same dimensions as the 19-hole circular polypropylene type except that the center hole was tapped to engage the threaded stud.

Figure 3.47 shows the pressure-time curve for this firing. The trace looks much like a conventional bulk-loaded firing. Muzzle velocity was slightly higher than for those shots in which plastic cavity generators were used at otherwise the same conditions. After the firing, the steel cavity generator was found to have broken loose from the stud and moved a short distance, a matter of a few inches. However, it is unlikely that it moved forward as rapidly or as far during the firing process as did its plastic counterparts.

Bulk-Loaded Firing

A firing was conducted with the chamber bulk loaded. The objective was to observe the characteristic bulk-loaded pressure-time curve for the igniter we are using in this series of tests. No cavity generator was used. The chamber was simply filled with propellant and fired using the same ignition system as had been used in other firings.

Figure 3.48 is the firing data for the bulk-loaded firing. The pressure time curve is characteristic of bulk-loaded firings in many guns. A high initial spike is followed by a plateau and then by expansion. Muzzle velocity was reasonably high at the expense of an extremely high pressure spike.

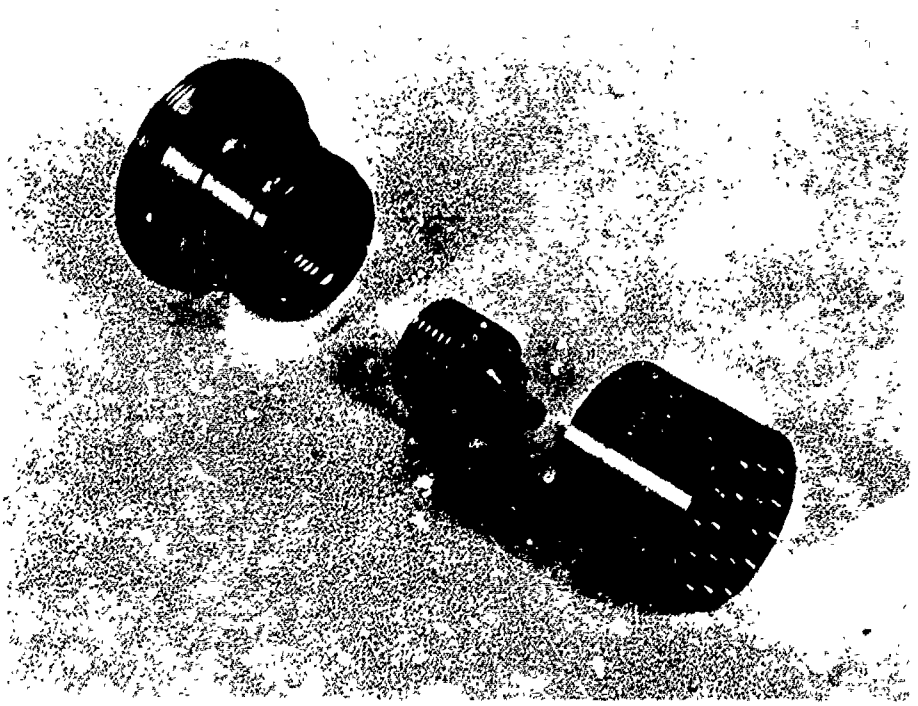

Figure 3.46. Photograph of Steel Orifice Plate

STEEL ORIFICE PLATE: 19 – .172 DIA HOLES
CIRCULAR
1 INCH LONG
SECURED TO BREECH
PH 13–8 Mo STAINLESS STEEL

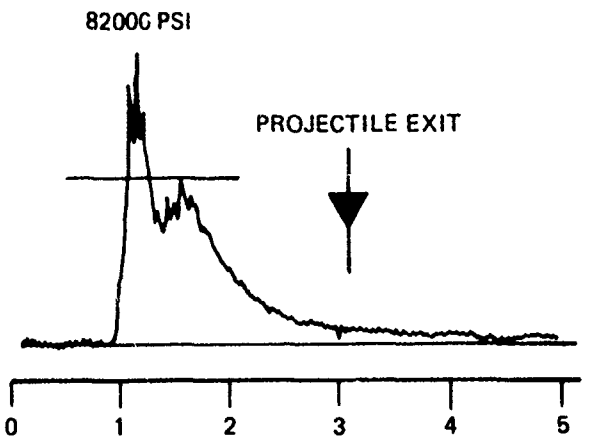

SHOT 30

TIME SCALE – MILLISECONDS

SHOT	Wp gm	Wc gm	C/M NOMINAL	A/A_c	Pc LB/IN^2	Vm FT/SEC
30	124.9	90	.75	.6	82000	4266 COILS 4533 SCREENS

Figure 3.47. Firing Data for Steel Orifice Plate

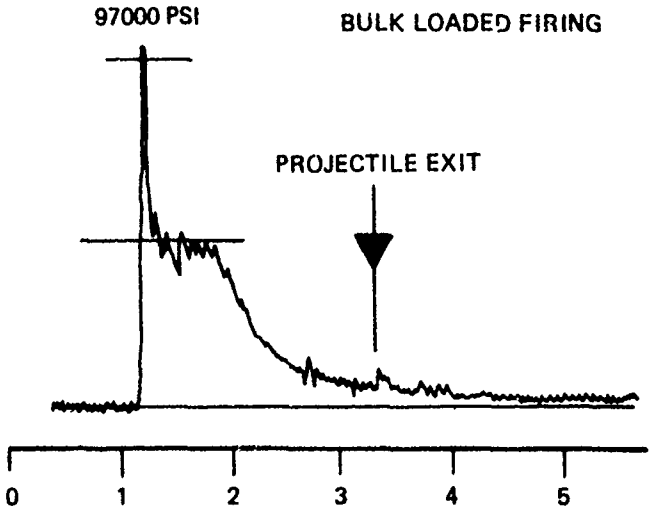

SHOT 33

TIME SCALE – MILLISECONDS

SHOT	Wp gm	Wc gm	C/M NOMINAL	A/A_c	Pc LB/IN^2	Vm FT/SEC
33	124.3	90	.75	.6	97000 PEAK 42000 PLATEAU	4787

Figure 3.48. Firing Data for Bulk Loaded Firing

3.3 Task 3 – Analysis Refinement

The area in which the original simplified analysis was least realistic was in the modeling of the burning rate. For lack of a more complete representation, the rate of gas evolution was assumed equal to the relative rate of flow of liquid charge back past the cavity generator. This is tantamount to assuming instantaneous burning as propellant passes through the plane in which lies the base of the cavity generator. Achieving a better representation of burning seemed the most logical task to approach first.

We considered various models for propellant burning. The cavity generator leaves a sheath of fluid along the wall, but it is not likely that this should be considered quiescent and burning only at the surface. It will undoubtedly break up under shear forces.

Nevertheless, a first step could be to assume that it doesn't break up but distributes itself in a uniform layer along the wall and burns in a linear manner outwardly from the inner cylindrical surface. The area of this surface will be proportional to circumference times length. Length is in turn a direct function of projectile travel.

An early version of the computation model was changed to make WGDOT, the rate of generation of gas, proportional to projectile travel as long as any liquid remained in the chamber:

$$WGDOT = Kx$$

where

WGDOT = Gas evolution rate - lb/sec
K = A constant whose value can be selected
x = Projectile travel

As K was varied, the character of the pressure-time curves and the manner in which propellant was consumed indeed changed. Muzzle velocity and peak chamber pressure changed as well. The exercise gave an indication that adjusting the burning rate will have a noticeable affect.

These results were interesting but they were still too preliminary. Straight proportionality to bullet travel is considered too elementary. A way was therefore sought to treat the unburned charge behind the cavity generator in a more realistic way. Some dependence on x should undoubtedly remain, but other effe ts such as relative velocities of liquid with respect to wall and cavity generator should be important as well.

A burning rate equation was next introduced which relates the net generation of gas to the amount of unburned liquid in the combustion zone, the chamber pressure to any desired power, and the relative velocity of gas and liquid as liquid is exposed to chamber gases behind the cavity generator. The velocity can also be raised to any desired power. The equation is

$$WGDOT = K*WLC*(PC)^{A}*(V1)^{B}$$

where

WLC	=	unburned liquid in combustion zone – lb
PC	=	chamber pressure – lb/in^2
V1	=	velocity of liquid relative to cavity generator at base · ft/sec
K,A,B	=	constants

The values of K, A, and B can be adjusted to desired values. Computations can be carried out to explore the relative effects of varying the constants.

As a preliminary check on this equation, some exploratory calculations were conducted with burning rate proportional only to WLC, the unburned propellant in the chamber in back of the cavity generator. Runs made with this dependence only, indicated that a fairly high value constant had to be assumed for appreciable chamber pressure to be generated. The more complete function, which relates burning rate to more than a simple proportionality to WLC, will probably be more realistic. A rough check of the constant showed that it compared in magnitude with that used for burning rate in the Foster-Miller report.*

The computation procedure was also altered to include propellant compressibility effects. Compressibility data from the latest NOS report was used in adjusting propellant density. Density is now calculated as a function of chamber pressure. This does not account for the density variation through the charge, which results from the inertial gradient, but such a refinement does not seem necessary yet. For one thing, we are extrapolating the NOS data to higher pressures than that for which it is reported, and in addition, the change in density at 50,000 PSI is only about 8%. Computations show that adding compressibility has a small effect. For the particular set of conditions checked, C/M = 0.5, A1/AC = 0.8, muzzle velocity increased 50 ft/sec from 3462 to 3512 ft/sec.

When testing began with the multiple hole cavity generators, a check was made between the test results and the adjusted analysis. Parameters were introduced which reflected the conditions of the firings at C/M = 0.5, 0.75, and 1.0 with polypropylene cavity generators. We found that the analysis does not successfully predict performance. This was true even when the burning rate was set equal to the liquid flow rate past the cavity generator, as had been assumed originally. In fact, the higher values of C/M produced lower predicted values of P_c and V_m. This occurred because as charge mass increases, acceleration decreases. Calculated injection rate decreases correspondingly and chamber pressure builds up more slowly. This trend was reflected to some degree in the overlay of Figure 3.4, where increasing C/M drove the predictions toward later burn out, not higher velocities.

*"Interior Ballistics of Liquid Propellant Guns", Alve Erickson, Foster-Miller Associates, 30 September 1973, Contract N00123-73-C-0278.

Comparison of calculated and observed values are tabulated below.

Table 3.7
Comparison of Predicted Performance and Test Results for
Multiple-Hole Polypropylene Cavity Generators

	Predicted by Analysis			Approximate Test Results	
	P_c	V_m	Burnout Travel	P_c	V_m
C/M	lb/in^2	ft/sec	in	lb/in^2	ft/sec
.50	47165	3713	46.75	59375	4300
.75	44578	3471	No Burnout	72000	4600
1.0	42556	3189	No Burnout	78750	5650

The reason for the lack of agreement is probably the limitation introduced into the analysis in assuming burning only behind the cavity generator. Observations suggest that burning apparently does occur ahead of the multi-hole cavity generators and that performance is best when it does so.

The analysis will require extension to include this effect.

4. CONCLUSIONS

The program outlined in the foregoing sections produced interesting results. Review of the data and reported observations leads to a number of conclusions:

1. The cavity generator concept achieves some control over the ballistic process in a bulk-loaded liquid propellant gun. The character of propellant ignition and the overall nature of the pressure-time curve were both shown to be sensitive to cavity generator design.
2. Hollow shell cavity generators produced a traveling charge effect. There was evidence that the charge carried far down bore in some firings and that liquid persisted along the wall for considerable time at some positions. However, satisfactory burning of the propellant was not realized. Delayed ignition and slow combustion were experienced with this type of cavity generator.
3. Thin shelled firings were not consistent. Continued slow burning was observed in some firings, and extremely rapid pressure rise late in the cycle was noted in others. Reasons for the contrast between such firings are not known.
4. The multiple hole cavity generator produced some excellent pressure-time curves and muzzle velocities. Muzzle velocity in some firings was higher than was expected on the basis of comparative data from other sources. Over 5500 feet per second was measured at a C/M ratio of 1.0. Apparently, an energy coupling effect exists which tends to improve performance under some circumstances.
5. Burning apparently takes place ahead of the cavity generator on many of the shots. The exact sequence of events through which this occurs is not yet known. Performance is best when burning does take place ahead of the cavity generator.
6. The transition of burning from the rear to the front of the multiple hole cavity generator seems to be a key factor in determining ignition characteristics and subsequent ballistic behavior.
7. The simplified analytical model in its present form does not successfully predict ballistic performance. This is not surprising, for the analysis does not model burning ahead of the cavity generator.
8. Pyrotechnic ignition of NOS 365 monopropellant offers no difficulty.
9. Obviously, much more needs to be learned about the cavity generator/traveling charge phenomena. Since further knowledge of cavity generator behavior may provide a key to the control of ballistics in bulk loaded guns, continued work is recommended.

5. RECOMMENDATIONS

The ability to achieve 5500 feet per second at C/M = 1.0 and with reasonable pressures is a very significant result. Additional experiments are warranted to better understand the underlying phenomena. The objective will be to ultimately develop practical means of controlling ignition and combustion in bulk loaded liquid propellant guns.

We therefore recommend that the firing tests be continued. Continuing the tests will involve the following steps:

- Revise and refurbish the test fixture.
- Add shot start.
- Redesign fill and vent valves.
- Redesign primer support for improved loading.
- Extend barrel length.
- Increase projectile weight to 186 gm (3000 grains).
- Conduct firing with various cavity generator configurations. The muzzle velocity of interest will be 5500 feet per second.
- Data analysis to formulate a theory which can explain the experimental results and form the basis for design.

APPENDIX 1

FIRING LOG

FIRING LOG – LIQUID PROPELLANT TRAVELING CHARGE GUN CONCEPT

Shot	Date	Projectile Type	W_p gm	W_c gm	$C/_M$ Nominal	Booster Charge	Cavity Generator	P_c lb/in^2	P_l lb/in^2
1	3-23	Teflon	120	60	.5	2.25gm Bullseye	SS shell, A_l/A_c = .8	7550 2600	2750 Second
2	3-24	Teflon	120	Water		2.25gm Bullseye	None		
3	3-25	Teflon	180	No Propellant		2.25gm Bullseye	None	4313	793
4	3-25	Teflon	120	60	.5	2.25gm Bullseye	SS shell, A_l/A_c = .8	7688 3180	3667 Second
5	3-26	Teflon	120	60	.5	1.9gm Bullseye	SS shell, A_l/A_c = .6	7125 8250	11500 Second
6	3-30	Teflon	120	60	.5	1.32gm Bullseye	SS shell, A_l/A_c = .4	7875 19688	12250 Second
7	4-1	Aluminum Lexan Skirt	112	60	.5	2.5gm Bullseye	SS shell, A_l/A_c = .6	9188 7125	8000 Second
8	4-1	Aluminum Lexan Skirt	112	60	.5	3.0gm Bullseye	SS shell, A_l/A_c = .6	14062 8438	7250 Second
9	4-9	Teflon	120	60	.5	.5cc NOS 365	SS shell, A_l/A_c = .6		20750
10	4-23	Teflon	120	60	.5	.25cc NOS 365	SS shell, A_l/A_c = .4	85000	20000
11	4-26	Teflon	121	60	.5	.25cc NOS 365	SS shell, A_l/A_c = .4	62500	11000
12	4-27	Aluminum Lexan Skirt	125.1	60	.5	.1cc NOS 365	SS shell, A_l/A_c = .4	111250	
13	4-27	Aluminum Lexan Skirt	115	60	.5	.25cc NOS 365	19 - .172 hole polypropylene circular 1 in. long, no skirt	43125 59375	 Second
14	5-12	Aluminum Lexan Skirt	115	120	1.0	.25cc NOS 365	19 - .172 hole polypropylene circular 1 in. long, attached skirt	78750	
15	5-13	Aluminum Lexan Skirt	123.2	60	.5	.10cc NOS 365	SS shell, A_l/A_c = .8		
16	5-14	Aluminum Lexan Skirt	123.2	60	.5	.25cc NOS 365	SS shell, A_l/A_c = .8	8750 5650	2250 Second
17	5-17	Aluminum Lexan Skirt	125.4	120	1.0	.25cc NOS 365	19 - .172 hole polypropylene circular 1 in. long, attached skirt		40000
18	5-18	Aluminum Lexan Skirt	125	120	1.0	.25cc NOS 365	19 - .172 hole polypropylene circular 1 in. long, attached skirt		33330
19	5-25	Teflon Cylinder	120	60 Water		.25cc NOS 365	None	6250	
20	5-25	Teflon Cylinder	120	120 Water		.25cc NOS 365	None	4000	
21	6-11	Aluminum Lexan Skirt	125	90	.75	.25cc NOS 365	19 - .172 hole polypropylene circular 1 in. long, attached skirt		40000
22	6-15	Aluminum Lexan Skirt	125.2	90	.75	.25cc NOS 365	19 - .172 hole polypropylene circular 1 in. long, attached skirt		25833

ity Generator	P_c lb/in^2	P_1 lb/in^2	P_2 lb/in^2	P_3 lb/in^2	P_4 lb/in^2	V_M ft/sec	Comments
hell, A_1/A_c = .8	7550	2750	2125	1250		1686	
	2600	Second	Peak				
e							Booster fired with water to study ignition.
e	4313	793				250	Booster fired with 180gm projectile to study ignition.
hell, A_1/A_c = .8	7688	3667	3167	1833		1841	1st light screen triggered early. V_M estimated from
	3180	Second	Peak				muzzle to 2nd screen.
hell, A_1/A_c = .6	7125	11500		7083		2435	Same as TC4.
	8250	Second	Peak				
hell, A_1/A_c = .4	7875	12250	16250	2500		2380	Light screens did not trigger properly. V_M estimated
	19688	Second	Peak				from microflash data.
hell, A_1/A_c = .6	9188	8000	8000	6000		2474	
	7125	Second	Peak				
hell, A_1/A_c = .6	14062	7250	6500	7250		2586	
	8438	Second	Peak				
hell, A_1/A_c = .6		20750	4250	1750		No data	Resembled bulk loaded firing.
hell, A_1/A_c = .4	85000	20000	4750	2000		3242	Resembled bulk loaded firing.
hell, A_1/A_c = .4	62500	11000	2500			4034	Polystyrene in nose of cavity generator.
							Double hump p-t curve.
hell, A_1/A_c = .4	111250		5000			4000	Delayed burning, rapid rise at 2 msec. V_M estimated,
							chronograph 4813 thought in error.
172 hole polypropylene	43125		6000	2000	1000	4305	Velocity coils added, double hump curve cavity
lar 1 in. long, no skirt	59375	Second	Peak				generator slivered and expelled from muzzle.
172 hole polypropylene	78750		17500	7500		5710	Cavity generator remained in bore
lar 1 in. long, attached skirt							
ell, A_1/A_c = .8							Misfire, reused cavity generator on next shot.
ell, A_1/A_c = .8	8750	2250	1250			1315	Delayed burning.
	5650	Second	Peak				
172 hole polypropylene		40000	17500		10250	5765	Cavity generator remained in bore.
ar 1 in. long, attached skirt							
172 hole polypropylene		33330	17500		10000	5545	Cavity generator remained in bore.
ar 1 in. long, attached skirt							
	6250						Water test of booster pressure.
	4000						Water test of booster pressure.
172 hole polypropylene		40000	18000	7500	5500	5300	Lost 1 coil, 1st light screen triggered early. V_M estimated
r 1 in. long, attached skirt							from 2nd coil and light screen. Spacing too close for accurate
							estimate.
72 hole polypropylene		25833		5000	3500	4942	
r 1 in. long, attached skirt							

FIRING LOG – LIQUID PROPELLANT TRAVELING CHARGE GUN CONCEPT

Shot	Date	Projectile Type	W_p gm	W_c gm	C/M Nominal	Booster Charge	Cavity Generator	P_c lb/in^2	P_1 lb/in^2	P_2 lb/in^2
23	6-16	Aluminum Lexan Skirt	124.8	90	.75	.25cc NOS 365	19 - .172 hole polypropylene circular 1 in. long, attached skirt			7500
24	6-21	Aluminum Lexan Skirt	125	90	.75	.25cc NOS 365	19 - .172 hole polypropylene circular 1 in. long, separate skirt	76250 7400	36000	5750
25	6-22	Aluminum Lexan Skirt	125	90	.75	.25cc NOS 365	19 - .172 hole polypropylene circular 1 in. long, separate skirt	70000 70000	24166	7500
26	6-28	Aluminum Lexan Skirt	124.3	90	.75	.25cc NOS 365	19 - .172 hole polypropylene circular 1 in. long, separate skirt	71000	25000	6500
27	6-30	Aluminum Lexan Skirt	125.4	90	.75	.25cc NOS 365	36 - .125 hole polypropylene circular 1 in. long, separate skirt	70000	20835	6250
28	6-30	Aluminum Lexan Skirt	125.4	90	.75	.25cc NOS 365	36 - .125 hole polypropylene circular 1 in. long, separate skirt	74000		8500
29	7-1	Aluminum Lexan Skirt O ring	125.6	90	.75	.25cc NOS 365	36 - .125 hole polypropylene circular 1 in. long, separate skirt	74000		
30	7-7	Aluminum Lexan Skirt O ring	124.9	90	.75	.25cc NOS 365	18 - .172 hole steel circular 1 in. long, attached to breech with center stud.	82000		
31	7-7	Aluminum Lexan Skirt O ring	124.2	90	.75	.25cc NOS 365	19 - .172 hole polypropylene circular 2 in. long, separate skirt	65000		
32	7-8	Aluminum Lexan Skirt O ring	123.8	90	.75	.25cc NOS 365	19 - .125 hole polypropylene hexagonal 1 in. long, separate skirt	62000		
33	7-8	Aluminum Lexan Skirt O ring	124.3	90	.75	.25cc NOS 365	None	97000 42000	Plateau	
34	8-10	Aluminum Lexan Skirt O ring	125	90	.75	.25cc NOS 365	19 - .172 hole polypropylene circular 2 in. long, separate skirt			
35	8-16	Aluminum Lexan Skirt O ring	125	90	.75	.25cc NOS 365	19 - .172 hole polypropylene circular 2 in. long, separate skirt	20000		
36	8-23	Aluminum Lexan Skirt O ring	125	90	.75	.25cc NOS 365	19 - .125 hole polypropylene hexagonal 1 in. long, separate skirt	76000		
37	8-23	Aluminum Lexan Skirt O ring	125	90	.75	.25cc NOS 365	19 - .125 hole polypropylene hexagonal 1 in. long, separate skirt	12000		
38	8-23	Aluminum Lexan Skirt O ring	125	90	.75	.25cc NOS 365	19 - .172 hole polypropylene hexagonal 1.375 long tapered holes, separate skirt	10000		
39	8-23	Aluminum Lexan Skirt O ring	125	90	.75	.25cc NOS 365	19 - .172 hole polypropylene hexagonal 1.375 long tapered holes, separate skirt	62000		
40	8-23	Aluminum Lexan Skirt O ring	125	90	.75	.25cc NOS 365	19 - .172 hole polypropylene hexagonal 1.375 long tapered holes, separate skirt	134000		

erator	P_c lb/in^2	P_1 lb/in^2	P_2 lb/in^2	P_3 lb/in^2	P_4 lb/in^2	V_M ft/sec	Comments
ole polypropylene n long, attached skirt			7500	4500	3000	4549	
ole polypropylene n. long, separate skirt	76250 7400	36000	5750		2500	4656	Two transducers for P_c. P_1 record doubtful.
ole polypropylene n. long, separate skirt	70000 70000	24166	7500		2500	4726	
ole polypropylene n. long, separate skirt	71000	25000	6500		3000	4591	
ole polypropylene n. long, separate skirt	70000	20835	6250	4500	4000	4407	P_1 record doubtful.
ole polypropylene n. long, separate skirt	74000		8500	6000	2500	4404	Down-bore pressure records doubtful.
ole polypropylene n. long, separate skirt	74000					4813	Down-bore pressures not recording properly. Not reported in subsequent shots. P_c record did not return to zero. O ring added to projectile for this and subsequent shots.
ole steel circular 1 in. ned to breech with .	82000					4266 4533	Chronograph failed to calculate V_M. Reported values for V_M calculated from coils, screens respectively.
ole polypropylene n. long, separate skirt	65000					3047	V_M calculated from coils. 1st light screen triggered early. Slower rise in P_c.
ole polypropylene 1 in. long, separate	62000					4637	Very nice p-t curve.
	97000 42000	Plateau				4787	Bulk loaded shot. Classic bulk loaded p-t curve.
ole polypropylene n. long, separate skirt						4400	Chronograph failed to calculate V_M properly. Pressure traces erratic.
ole polypropylene n. long, separate skirt	20000					1385	Peak P_c obscured by fire volts pulse. Propellant expelled from muzzle. V_M calculated from coils. Difficulty sealing cavity generator. Ignition delay less than .2 msec.
ole polypropylene 1 in. long, separate	76000					4771	P_c trace did not return to zero. V_M calculated from coils.
ole polypropylene 1 in. long, separate	12000					1472	Low pressure shot.
ole polypropylene 1.375 long les, separate skirt	10000					1535	Low pressure shot.
ole polypropylene 1.375 long les, separate skirt	62000					2105	Erratic P_c trace.
ole polypropylene 1.375 long es, separate skirt	134000					4266	Delayed ignition followed by high spike. V_M from coils, screens did not record properly. Damage to primer support. Primer ruptured.

APPENDIX 2

BARREL DIMENSIONAL CHANGE

The chamber region was subjected to some high pressures during the test program. To determine whether bore enlargement had occurred, a measurement survey was made after the tests concluded. The relative contributions of corrosion or erosion, if they occurred, are not known. The following table summarizes the measurement of bore diameter at the conclusion of the test.

Station	Diameter
2.50	1.202
3.50	1.206
4.50	1.202
5.50	1.200
6.50	1.202
7.50	1.204
8.50	1.206
9.50	1.199
10.50	1.191
11.50	1.189
16.50	1.185
26.50	1.185
36.50	1.184
46.50	1.185
56.50	1.185
66.50	1.187
76.50	1.185
86.50	1.186
Original Diameter	1.184